

Functional characterization of a glutamate
transporter from *Escherichia coli*

Ivanna Shcherbyna

Functional characterization of a glutamate
transporter from *Escherichia coli*

Von der Naturwissenschaftlichen Fakultät
der Gottfried Wilhelm Leibniz Universität Hannover
zur Erlangung des Grades

Doktorin der Naturwissenschaften

-Dr. rer. nat.-

genehmigte Dissertation

von

Ivanna Shcherbyna, Magistr Diplom,
geboren am 20. Januar 1976, in Kiew, Ukraine

2009

Referent: Prof. Dr. Christoph Fahlke

Korreferent: Prof. Dr. Anaclet Ngezahayo

Tag der Promotion: 12-August-2009

Dedicated to my dear sister
Oleksandra

Contents

1. Introduction.....	1
1.1 Neurotransmitter transporters.....	2
1.2 L-glutamate as a neurotransmitter.....	3
1.2.1 Role of glutamate uptake in disease.....	4
1.3 Glutamate transporters.....	5
1.3.1 Mammalian glutamate transporters (EAAT family).....	6
1.3.2 Bacterial glutamate transporters.....	9
1.3.3 Stoichiometry.....	10
1.3.4 Structure.....	11
1.4 Aim of the thesis.....	16
2. Materials and methods.....	17
2.1 Chemicals, materials and equipment.....	18
2.1.1 Materials and equipment.....	18
2.1.2 Chemicals.....	18
2.2 Molecular biology.....	19
2.2.1 Sequence alignments.....	19
2.2.2 Plasmids.....	19
2.2.3 Mutagenesis.....	19
2.2.3.1 Primers and resulting constructs.....	19
2.2.3.2 Polymerase Chain Reaction.....	20
2.2.3.3 Quikchange method.....	21
2.2.4 Transformation.....	22

2.2.5 Plasmid recovery / purification / storage.....	22
2.2.6 DNA concentration measurement.....	23
2.2.7 Agarose gel electrophoresis.....	23
2.2.8 DNA Restriction Enzymes.....	23
2.2.9 Gel extraction.....	24
2.2.9.1 Glass milk preparation.....	25
2.2.10 Ligation.....	25
2.2.11 DNA sequencing.....	25
2.2.11.1 Ethanol precipitation of sequenced DNA.....	26
2.2.12 LB medium, agar plates and antibiotics.....	26
2.2.13 Competent bacteria.....	26
2.3 Protein biochemistry.....	27
2.3.1 Expression of ecglP.....	27
2.3.2 Bacteria lysis and membrane pellet preparation.....	28
2.3.3 Solubilization of ecglP from the membrane pellet.....	28
2.3.4 Purification of ecglP by affinity chromatography.....	28
2.3.5 Size-exclusion chromatography.....	29
2.3.6 SDS-PAGE analysis.....	30
2.4 Functional assays.....	30
2.4.1 ecglP reconstitution protocol.....	30
2.4.2 L-[³ H]-glutamate / L-[³ H]-aspartate uptake.....	31
2.4.3 Data analysis.....	33
3. Results.....	34
3.1 ecglP protein purification.....	35
3.2 Purified and reconstituted ecglP mediates substrate transport into proteoliposomes.....	37

3.2.1	Glutamate accumulation by proteoliposomes containing purified ecglTP.....	37
3.2.2	Substrate specificity of ecglTP.....	38
3.3	Cation selectivity of ecglTP.....	39
3.3.1	Glutamate uptake by ecglTP is sodium- and potassium-independent.....	39
3.3.2	ecglTP co-transporters glutamate and H ⁺	40
3.4	Determination of the transport stoichiometry of ecglTP.....	41
3.4.1	Electrogenicity of glutamate transport by ecglTP.....	41
3.4.2	Determination of the coupling stoichiometry of ecglTP by the static head method.....	42
3.4.3	Determination of the coupling stoichiometry of ecglTP by voltage dependence measurements.....	44
3.5	Temperature dependence of ecglTP-mediated glutamate uptake.....	46
3.6	Characterization of N401D ecglTP.....	47
3.6.1	N401D ecglTP mediates glutamate/aspartate transport into liposomes.....	47
3.6.2	N401D ecglTP mediates electrogenic co-transport of substrate and protons	48
3.6.3	Aspartate uptake by N401D ecglTP is Na ⁺ -independent.....	49
3.6.4	Determination of the coupling stoichiometry of N401D ecglTP by voltage dependence measurements.....	50
4.	Discussion.....	52
4.1	Purified and reconstituted ecglTP mediates glutamate uptake into proteoliposomes.....	53
4.2	ecglTP has less substrate specificity than eukaryotic EAAT glutamate transporters.....	54

4.3 Stoichiometry of ecglTP: three protons are electrogenically co-transported with one glutamate.....	54
4.4 Determination of unitary transport rates and temperature dependence of ecglTP-mediated glutamate uptake.....	55
4.5 Characterization of N401D ecglTP.....	57
4.6 Conclusions.....	58
4.7 Further research.....	59
5. Abstract.....	60
5.1 Abstract, English.....	61
5.2 Zusammenfassung.....	62
6. References.....	63
7. Supplemental Information.....	76
8. Acknowledgements.....	83
9. Curriculum Vitae.....	84
10. List of publications.....	85

List of Figures and Tables

Figures

1.1 Chemical structure of L-glutamate.....	3
1.2 Phylogenetic tree of 35 members of the DAACS family (Slotboom <i>et al.</i> , 1999).	6
1.3 Phylogenetic tree of some mammalian members of the glutamate transporter family.....	7
1.4 Simplified view of the signal transmission between two excited nerve cells by the neurotransmitter glutamate and its removal from the synaptic cleft via glutamate transporters (EAATs).....	8
1.5 Stoichiometry of glutamate transporters.....	10
1.6 Phylogenic relationship of three distantly related glutamate transporters Glt _{ph} , ecgltP, and hEAAT2.....	12
1.7 Sequence identities of three distantly related glutamate transporters Glt _{ph} , ecgltP, and hEAAT2.....	13
1.8 Crystal structure of a bacterial glutamate transporter Glt _{ph} from <i>Pyrococcus horikoshii</i> (Yernool <i>et al.</i> , 2004).....	14
1.9 Protomer.....	14
1.10 Localization of the N401D mutation.....	16
2.1 Scheme of the Quikchange reaction.....	21
2.2 Solubilization of liposomes.....	31
2.3 Schematic demonstrations of ecgltP reconstitution in lipid vesicles and the uptake experiment.....	32
3.1 Overexpression and purification of ecgltP.....	35
3.2 Purified ecgltP.....	36
3.3 Affinity and size-exclusion chromatography elution profiles of ecgltP.....	36
3.4 Purified and reconstituted ecgltP mediates glutamate transport into liposomes....	37

3.5 Protein concentration-dependence of the transport rate (A) and accumulation (B) of L-[³ H]-glutamate into ecglpP proteoliposomes.....	38
3.6 L-[³ H]-glutamate uptake in the presence of various non-radioactive substrates at a concentration of 500 μM.....	38
3.7 Uptake levels of 0.0175 μM L-[³ H]-glutamate, L-[¹⁴ C]-serine and [³ H]- dopamine.....	39
3.8 L-[³ H]-glutamate uptake at various concentrations of extravesicular Na ⁺ (A) or intravesicular K ⁺ (B)	40
3.9 ecglpP co-transporters glutamate and H ⁺	41
3.10 Valinomycin structure.....	41
3.11 Glutamate transport by ecglpP is electrogenic.....	42
3.12 Static head experiment.....	44
3.13 Voltage dependence of glutamate transport by ecglpP.....	45
3.14 Coupling stoichiometry of ecglpP.....	45
3.15 Temperature dependence of ecglpP glutamate transport.....	46
3.16 Arrhenius plot for initial transport rates.....	46
3.17 Substrate transport into proteoliposomes via N401D ecglpP.....	47
3.18 N401D ecglpP co-transporters aspartate and H ⁺	48
3.19 L-[³ H]-aspartate uptake via N401D ecglpP at various concentrations of extravesicular Na ⁺	49
3.20 The voltage dependence of glutamate transport by N401D ecglpP.....	50
3.21 Coupling stoichiometry of WT ecglpP and N401D ecglpP.....	50

Tables

2.1 Constituents of the running and stacking SDS gels.....	30
7.1 Members of the of the DAACS family.....	76
7.2 Score Table of three distantly related glutamate transporters Glt _{Ph} , ecgltP, and hEAAT2.....	76
7.3 List of equipment and materials used.....	77
7.4 List of chemicals used.....	79
7.5 Oligonucleotides used.....	82
7.6 Used <i>Escherichia coli</i> -strain	82

Abbreviations

aa	amino acid
AHT	anhydrotetracycline hydrochloride
AMPSO	N-(1,1-Dimethyl-2-hydroxyethyl)-3-amino-2 hydroxypropanesulfonic acid
APS	ammonium persulphate
ASCTA	alanine serine cysteine transporter
bp	base pairs
BSA	bovine serum albumin
CNS	central nervous system
CPM	counts per minute
CV	column volume
DAACS	sodium/dicarboxylate amino acid cation symporters
dATP	2'-deoxyadenosine 5'-triphosphate
DDM	n-Dodecyl- β -maltoside
dG	Gibb's free energy
DMF	dimethylformamide
DMSO	dimethylsulfoxide
DNA	deoxyribonucleic acid
dNTPs	deoxyribonucleotide triphosphates
DPM	disintegrations per minute
DTT	dithiothreitol
<i>E. coli</i>	<i>Escherichia coli</i>
EAAT	excitatory amino acid transporter
ecglTP	glutamate transporter from <i>Escherichia coli</i>
EDTA	ethylenediaminetetraacetic acid, anhydrous
EGTA	ethylene glycol-bis(2-aminoethyl ether)-N,N,N',N'-tetraacetic acid
E_K	K^+ equilibrium potential
e_0	elementary charge
F	Faraday's constant ($9.648 \cdot 10^4$ Coulombs mol ⁻¹)
Fig.	figure
FPLC	fast protein liquid chromatography
g	g-force

Abbreviations

GABA	gamma-aminobutyric acid
Glt _{ph}	glutamate transporter from <i>Pyrococcus horikoshii</i>
GPC	gel-filtration or gel-permeation chromatography
h	hour
HABA	4'-Hydroxyazobenzene-2-carboxylic acid
HEPES	4-(2-hydroxyethyl)-1-piperazine ethanesulfonic acid
HPLC	high pressure liquid chromatography / high performance liquid chromatography
k	Boltzmann constant
kbp	kilobase pairs
kDa	kilodalton
LB medium	Luria-Bertani medium
LDAO	lauryldimethylamine-oxide
LMW	low molecular weight marker
M	mole
MES	morpholinoethanesulfonic acid
mg/ml	milligram per milliliter
min	minute
ml	milliliter 1 ml=10 ⁻³ liter
mm	millimeter
MOPS	3-(N-morpholino)propanesulfonic acid
mV	millivolt
MW	molecular weight
ng	nanogram
nm	nanometer
NMDG	N-methyl-D-glucamine
NSS	neurotransmitter sodium symporter family
OD	optical density
ON	overnight
p	significance
PBS	phosphate buffer saline
PCR	polymerase chain reaction
pH _i	intravesicular pH
pH _o	extravesicular pH

Abbreviations

PIPES	piperazine-N,N'-bis(2-ethanesulfonic acid)
PMSF	phenylmethylsulphonylfluoride
<i>P. horikoshii</i>	<i>Pyrococcus horikoshii</i>
R	Gas constant ($8.315 \text{ J}^{-1} \text{ K}^{-1} \text{ mol}^{-1}$)
rpm	revolutions per minute
RT	room temperature
SAM	s-adenosyl methionine
SDS	sodium dodecylsulphate
SDS-PAGE	sodium dodecylsulphate polyacrylamide gel electrophoresis
sec	second
SEC	size-exclusion chromatography
T	absolute temperature
t	time
T _A	annealing temperature
Tab.	table
TAE	Tris-acetate-EDTA buffer
TCEP	tris(2-carboxyethyl)phosphine hydrochloride
TEA	tetraethyl ammonium
TEMED	N,N,N'-tetramethyl-ethylene diamine
T _m	melting temperature
TRIS	tris(hydroxymethyl)-aminomethane
U	1 enzyme unit = $16.67 \cdot 10^{-9} \text{ kat} = 16.67 \text{ nkat}$
UV	ultraviolet light
V	voltage
v/v	volume per volume
V _o	void volume
w/v	weight per volume
WT	wild type
°C	degree Celsius
µg	microgram
µl	microliter
µm	micrometer
µM	micromolar

1. Introduction

1.1 Neurotransmitter transporters

The neuronal communication in the nervous system relies on the action of neurotransmitters at chemical synapses between neurons. An action potential promotes the release of the neurotransmitter, increasing its concentration 10^3 – 10^4 -fold in the synaptic cleft. After being released, neurotransmitters specifically bind to postsynaptic receptors and thereby activate them. The neurotransmitter opens ligand-gated ion channels, resulting in depolarization of the postsynaptic neuron and the generation of a postsynaptic receptor potential. This process, depending on the receptor type, leads to excitation or inhibition of the postsynaptic neuron. Intercellular communication in the central nervous system (CNS) requires the precise control of the duration and intensity of the neurotransmitter action. This regulation occurs via the inactivation of the transmitter, either by enzymatic degradation or active transport by neurotransmitter transporters. At many synapses integral membrane transport proteins located on presynaptic, postsynaptic and glial cells clear the transmitter from the synaptic cleft, reducing the concentration of transmitter to the basal level, thereby readying the synapse for a subsequent cycle of activation (Clements, 1996). The superfamily of plasma membrane transporters (Masson *et al.*, 1999) can be classified into two distinct families based on their ionic dependency. The first is the neurotransmitter sodium symporter family (NSS), which consists of Na^+/Cl^- -dependent transporters including, for example, transporters for dopamine (DAT), serotonin (5-HT, SERT), GABA [GAT(1-3)], norepinephrine (NET), proline (PROT), taurine (TaurT), and glycine [GLYT(1a, -b, -c, and -2)]. All NSS proteins share the same topology and are 40 % to 60 % homologous to one another. The second family of the plasma membrane transporters is the family of sodium/dicarboxylate amino acid cation symporters (DAACS), which contains the eukaryotic Na^+/K^+ -dependent glutamate transporters (excitatory amino acid transporters 1 to 5, or EAATs) and also includes prokaryotic glutamate, dicarboxylate and serine transporters. This study focuses on members of this last group, the glutamate transporters. The following sections will briefly introduce the relevant glutamate transporters existing in eukaryotes and their prokaryotic paralogs. As glutamate is the predominant neurotransmitter in many excitatory pathways of the mammalian CNS, understanding the mechanisms underlying coupled transport by glutamate transporters has high importance and was the target of this work.

1.2 L-glutamate as a neurotransmitter

The amino acid L-glutamate (Fig. 1.1), abbreviated as Glu or E, is a non-essential amino acid in vertebrates. It serves as a component of protein synthesis, energy metabolism and as predecessor for glutamine and also functions as the major excitatory neurotransmitter in the mammalian CNS (Fonnum, 1984; Cotman *et al.*, 1987; Robinson *et al.*, 1987; Takeuchi, 1987).

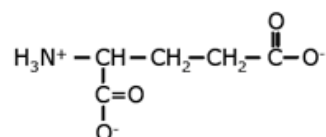


Figure 1.1 Chemical structure of L-glutamate.

Glutamate is ubiquitously distributed in brain tissue, where it is present in high concentrations in comparison to other amino acids. Glutamate is involved in most processes and aspects of normal brain function, including memory, learning and cognition (Fonnum, 1984; Danbolt, 2001). Glutamate also plays major roles in many processes during CNS development, including neuronal migration (Rossi *et al.*, 1993; Komuro *et al.*, 1993) and GABAergic activity (van den Pol *et al.*, 1998), as well as outgrowth of neuronal processes (Pearce *et al.*, 1987). Furthermore, glutamate is important for synapse elimination (Rabacchi *et al.*, 1992), and for functional synapse induction in the developing nervous system and also for long-term potentiation (Durand *et al.*, 1996).

Brain glutamate is abundant, but mostly intracellular. The concentration gradient of glutamate across the plasma membranes has a magnitude of several thousand, with the highest concentrations found inside nerve terminals (Danbolt, 2001). Glutamate is continuously being released from cells and again removed from the extracellular fluid. Upon production of the action potential, L-glutamate is released from the presynaptic neuron into the synaptic cleft. After its release, the concentration of glutamate in the synaptic cleft rises from 1 μM to 1 mM and elicits the postsynaptic answer through interaction with glutamate receptors. Synaptic release of glutamate may activate several ionotropic and metabotropic receptors to mediate a complex array of functions. Glutamate taken up by pre- and postsynaptic cells may be used for metabolic purposes such as protein synthesis and energy metabolism; in pre-synaptic cells it also may be reused as a transmitter (Danbolt, 2001). Glutamate taken

up by glial cells can be converted to glutamine in an ATP-dependent process (glutamate-glutamine cycle) (Broer *et al.*, 2001). Glutamine is subsequently released from the glial cells and taken up by neurons via glutamine transporters. Neurons convert glutamine back to glutamate, which is then transported into the synaptic vesicles by vesicular glutamate transporters (Broer *et al.*, 2001).

Glutamate is a neurotoxin. At concentrations between 50 μM and 100 μM glutamate causes cell death after 5 minutes. Already after 90 seconds glutamate application produces the first morphologic changes in adult neurons (Choi *et al.*, 1987). It is therefore crucial that the resting extracellular glutamate concentration remains low. This is required for a high signal to background ratio in synaptic transmission and also for the protection of nerve cells from the toxic effects of glutamate. Considering the large amounts of glutamate in the brain and the importance of controlling the extracellular glutamate concentrations after its release, the CNS needs powerful protective machinery to prevent extracellular glutamate accumulation. In contrast to extracellular glutamate, intracellular glutamate is generally considered non-toxic (Danbolt, 2001). Finally, to conserve resources it is practical to reuse the released glutamate. Glutamate is removed by the neuronal and glial glutamate transporters, which Arriza *et al.* (1994) have termed „Excitatory Amino Acid Transporters“ (EAATs). Members of the EAAT family tightly control the glutamate concentration in the synaptic cleft (Billups *et al.*, 1996; Kanner, 1996; Danbolt, 2001; Amara *et al.*, 2002). EAATs are located in presynaptic, postsynaptic and glial cells and they rapidly remove glutamate from the synaptic cleft and the perisynaptic area.

1.2.1 Role of glutamate uptake in disease

Brain tissue needs a very high glutamate uptake activity to protect itself against glutamate toxicity because there is no extracellular conversion of glutamate (Danbolt, 2001), as there is for example for acetylcholine. Removal of glutamate from the synaptic cleft has high importance for two reasons: (1) the neurotoxicity of glutamate and (2) the necessity of exact and accurate regulation of signal transduction by the inactivation of glutamate (Danbolt, 2001). Rapid clearance of glutamate from the synapse by high-affinity sodium-dependent EAATs is required for normal excitatory neurotransmission and for the prevention of glutamate-induced excitotoxicity (Bergles *et al.*, 1999; Danbolt, 2001). Failure in EAAT function

provokes neuro-excitotoxicity by elevation of the extracellular glutamate concentration, causing excessive stimulation of the glutamate receptors that, if prolonged, will result in processes leading to cell death (Rossi *et al.*, 2000). A link between glutamate transporter dysfunction, increased extracellular glutamate level, and the onset of excitotoxic neuronal damage has been established in animal models (Rothstein *et al.*, 1996) and in some human neurodegenerative diseases such as amyotrophic lateral sclerosis (ALS) (Rothstein *et al.*, 1992; Rothstein *et al.*, 1995; Howland *et al.*, 2002), Alzheimer's disease (Scott *et al.*, 1995; Scott *et al.*, 2002), apoplexy (Rothman, 1984), epilepsy (Nadler *et al.*, 1978), schizophrenia, and depression (Dingledine *et al.*, 1999). For this reason it is of high importance to study and understand the mechanisms underlying glutamate uptake by glutamate transporters.

1.3 Glutamate transporters

Glutamate transporters belong to the DAACS family (see section 1.1), which includes eukaryotic glutamate transporters, eukaryotic neutral amino acid transporters, and a large number of bacterial amino acid and dicarboxylic acid transporters (Slotboom *et al.*, 1999; Danbolt, 2001; Kanai *et al.*, 2003). Members of this family that have been functionally characterized can be classified into three groups based on their substrate specificity: (1) C4-dicarboxylate transporters found in prokaryotes, (2) glutamate/aspartate transporters found in prokaryotes and eukaryotes and (3) neutral amino acid transporters found in prokaryotes and eukaryotes (Slotboom *et al.*, 1999). The phylogenetic tree of the DAACS family is presented in Fig. 1.2.

All glutamate transporters can use L-glutamate, L-aspartate and D-aspartate as high-affinity substrates. The bacterial C4-dicarboxylate transporters transport succinate, fumarate, and malate, thereby contributing to the citric acid cycle (Finan *et al.*, 1981; Finan *et al.*, 1988). This group of transporters shares up to 40 % amino acid sequence identity with each other. Alanine, cysteine, serine, and threonine are high affinity substrates of the neutral amino acid transporters. Some members of this group show lower substrate specificity and also accept glutamine and asparagine with higher affinity, and some other amino acids with lower affinity (Arriza *et al.*, 1993; Tamarappoo *et al.* 1996; Utsunomiya-Tate *et al.*, 1996; Kekuda *et al.*, 1996; Kekuda *et al.*, 1997).

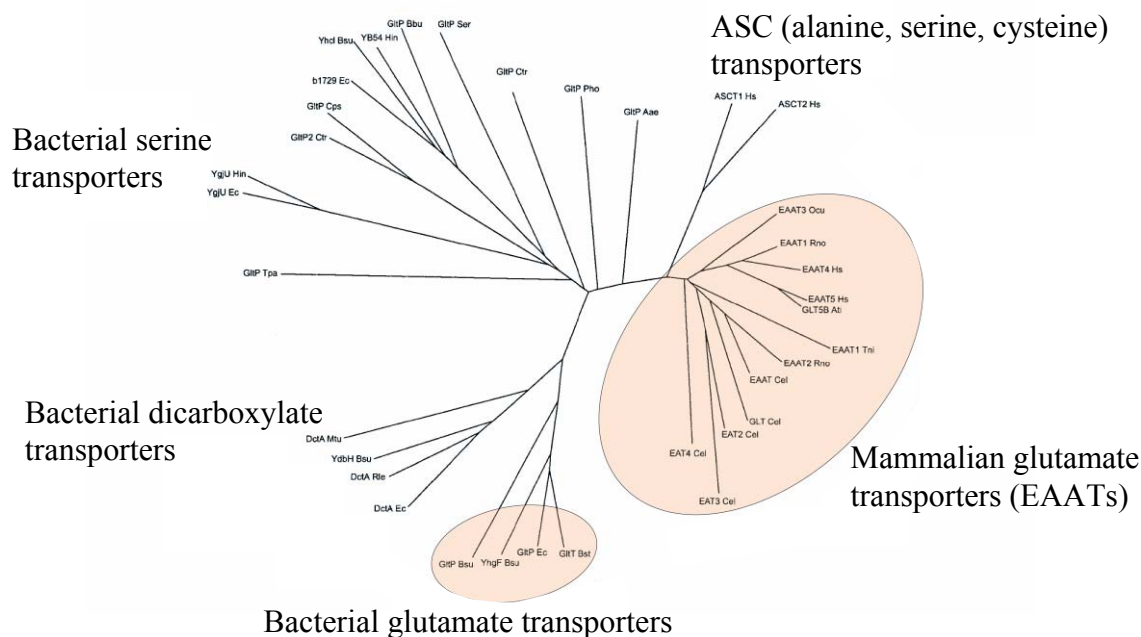


Figure 1.2 Phylogenetic tree of 35 members of the DAACS family (Slotboom *et al.*, 1999). The tree is based on the part of the multiple-sequence alignment (Slotboom *et al.*, 1999). No members of the set have higher than 70 % amino acid identity to one another. Abbreviated transporter names are shown in Table 7.1.

1.3.1 Mammalian glutamate transporters (EAAT family)

Excitatory amino acid transporters (EAATs) remove glutamate from the synaptic cleft to ensure low resting glutamate concentrations and to terminate glutamatergic synaptic transmission. Five different mammalian high-affinity sodium-dependent glutamate transporters (EAAT1-5) have been cloned so far. EAAT1, 2 and 3 were cloned from human motor cortex (Storck *et al.*, 1992; Pines *et al.*, 1992; Kanai *et al.*, 1992; Arriza *et al.*, 1994). EAAT4 was cloned from human cerebellum (Fairman *et al.*, 1995) and EAAT5 was cloned from human retina (Fairman *et al.*, 1995; Arriza *et al.*, 1997). Figure 1.3 shows the phylogenetic tree of some members of this family.

Only the human isoforms of the excitatory amino acid transporters are termed EAATs, homologues in other species that were in some cases cloned earlier are GLAST (Glutamate Aspartate Transporter, rat equivalent of human EAAT1) (Storck *et al.*, 1992), GLT1 (Glutamate Transporter 1, rat equivalent of human EAAT2) (Pines *et al.*, 1992) and EAAC1 (Excitatory Amino Acid Carrier 1, rabbit equivalent of human EAAT3) (Kanai *et al.*, 1992). The five cloned EAAT glutamate transporters

share 50 % to 60 % amino acid sequence identity with each other, and typically have 30 % to 40 % identity to transporters for neutral amino acids (Arriza *et al.*, 1993), and 20 % to 30 % identity to proton-dependent bacterial glutamate and dicarboxylate transporters (Tolner *et al.*, 1992; Danbolt, 2001). Among mammals, the five cloned glutamate transporter subtypes are approximately 90 % identical to their homologues in different species (Danbolt, 2001).

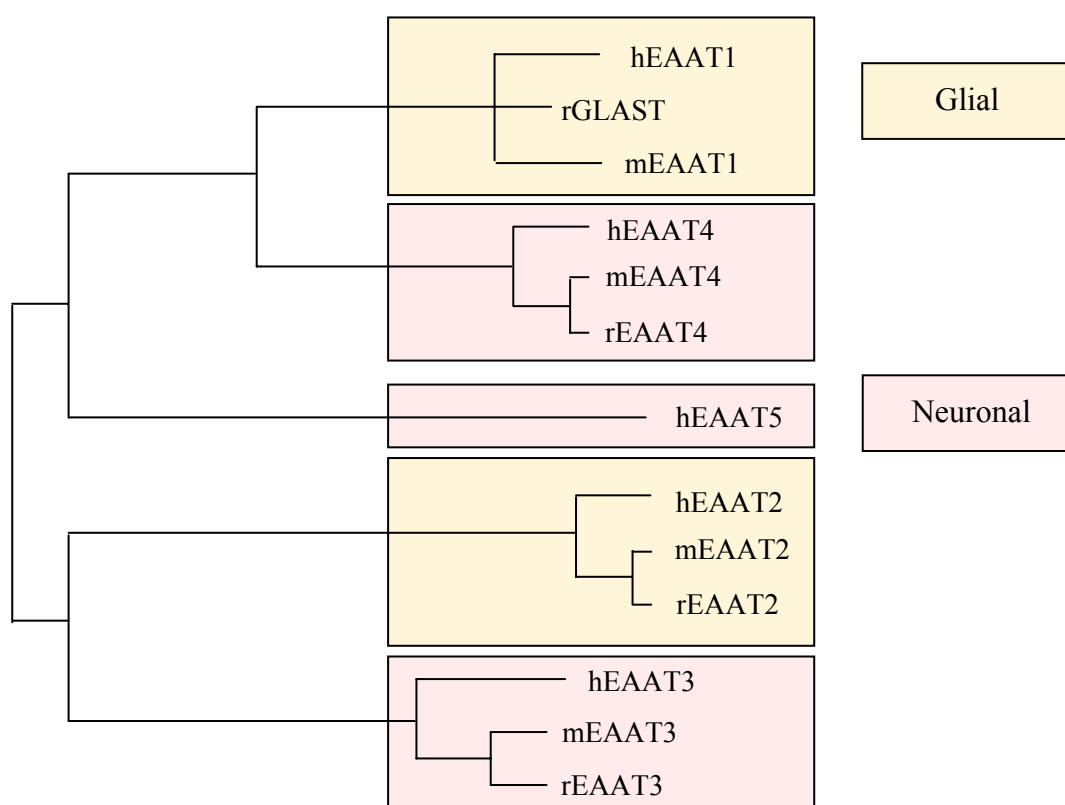


Figure 1.3 Phylogenetic tree of some mammalian members of the glutamate transporter family.

Glial glutamate transporters: hEAAT1 (Arriza *et al.*, 1994; Larsson *et al.*, 1996), rGLAST (Storck *et al.*, 1992; Larsson *et al.*, 1996), mEAAT1 (Tanaka, 1993), hEAAT2 (Arriza *et al.*, 1994), mEAAT2 (Kirschner *et al.*, 1994), rEAAT2 (Pines *et al.*, 1992). Neuronal glutamate transporters: hEAAT4 (Fairman *et al.*, 1995), mEAAT4 (Maeno-Hikichi *et al.*, 1997), rEAAT4 (Lin *et al.*, 1998), hEAAT5 (Arriza *et al.*, 1997), hEAAT3 (Arriza *et al.*, 1994), mEAAT3 (Mukainaka *et al.*, 1995), rEAAT3 (Kanai *et al.*, 1995; Larsson *et al.*, 1996). Abbreviations: human (h), mouse (m), and rat (r) isoforms.

All five EAATs proteins catalyze H^+ -, Na^+ - and K^+ -coupled transport of L-glutamate and also of L- and D-aspartate. Originally, these transporters were referred to as the “sodium-dependent high-affinity transporters” to distinguish them from the “low-affinity transporters”. “Low-affinity” uptake has K_m values of above 500 μM and, in contrast to the “high affinity system”, is sodium independent and sensitive to inhibition by D-glutamate and L-homocysteate. This uptake system has been

suggested to supply brain cells with amino acids for metabolic purposes, but is poorly characterized (Danbolt, 2001).

The neurotransmission of the signal and cell specific expression of the five EAATs are schematically demonstrated in simplified view of two excited nerve cells (Fig. 1.4).

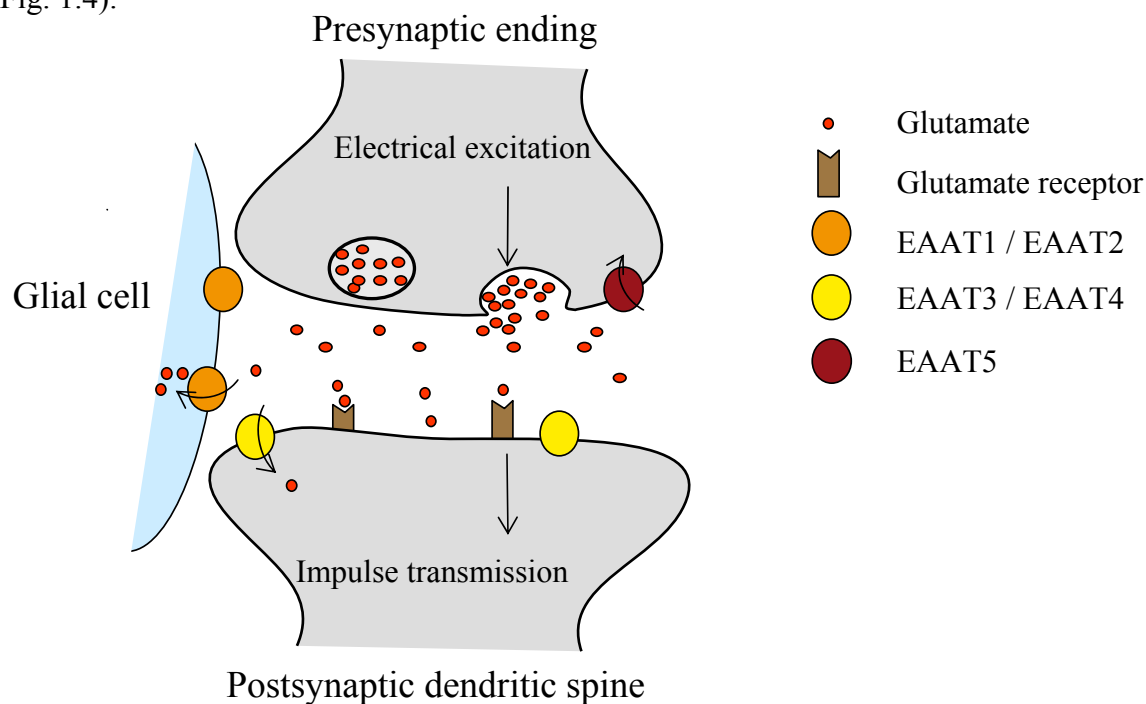


Figure 1.4 Signal transmission between two excited nerve cells by the neurotransmitter glutamate and its removal from the synaptic cleft via glutamate transporters (EAATs).

The localization of EAATs is well known. EAAT2 is the main glial glutamate transporter and the most abundant isoform in the forebrain (Danbolt *et al.*, 1992; Rauen, 2000). EAAT1 is a glial glutamate transporter, expressed in astrocytes and Bergmann glia in the cerebellum (Storck *et al.*, 1992; Rothstein *et al.*, 1994). EAAT3 is homogeneously distributed throughout the CNS. It is the predominant EAAT expressed in neurons of various brain areas, particularly in the thalamus, cerebellum, hippocampus, olfactory bulb, and striatum (Rothstein *et al.*, 1994; Kanai *et al.*, 1995; Berger *et al.*, 1998). EAAT4 is the main cerebellar glutamate transporter, specifically in the Purkinje cells (Yamada *et al.*, 1996; Furuta *et al.*, 1997; Dehnes *et al.*, 1998; Inage *et al.*, 1998). A study using electron microscopy found the majority of the EAAT4 immunoreactivity in the plasma membrane of Purkinje cells and that the highest levels are extra-synaptic (Dehnes *et al.*, 1998). Very little is known about EAAT5. This isoform seems to be retina-specific (Arriza *et al.*, 1997; Eliasof *et al.*, 1998a; Eliasof *et al.*, 1998b). It is present in both cone and rod photoreceptors as well

as in amacrine, ganglial (Fyk-Kolodziej *et al.*, 2004), bipolar and Müller cells (Eliasof *et al.*, 1998b).

Glutamate uptake also takes place in peripheral tissues and organs. Most cells and tissues have the ability to take up glutamate. Sodium-dependent glutamate uptake systems have been identified in fibroblasts from various tissues, in erythrocytes, macrophages, platelets, muscles, prostate, liver, taste buds, mammalian oocytes, the intestine, kidney, pancreas, placenta, heart, bone and mammary gland (Danbolt, 2001).

1.3.2 Bacterial glutamate transporters

Bacterial glutamate transporter proteins are nutritional transporters. Thus, in prokaryotes, glutamate transporters carry out the concentrative uptake of metabolites across the membrane by the co-transport of protons and/or sodium ions (Slotboom *et al.*, 1999).

Prokaryotic glutamate transporters are only distantly related to eukaryotic glutamate transporter isoforms (Fig. 1.2). Bacterial glutamate transporter proteins have more than 44 % amino acid homology and transport at least two cations in symport with glutamate (Tolner *et al.*, 1992; Tolner *et al.*, 1995a; Tolner *et al.*, 1995b). In *Escherichia coli* (*E. coli*) internalised glutamate is used as a carbon and nitrogen source (Halpern *et al.*, 1965). As far as is known, *E. coli* has three different systems to take up glutamate: (1) a sodium-independent protein-dependent glutamate- and aspartate transport system, which is inhibited by cysteate (Halpern *et al.*, 1973), (2) a sodium-dependent glutamate specific system (ecgltS), inhibited by α -methyl hydrate (Miner *et al.*, 1974), and (3) a proton symport system for glutamate and aspartate (ecgltP), inhibited by o-hydroxy aspartate and cysteate (Schellenberg *et al.*, 1977). This study focuses on this last protein, ecgltP from *E. coli*.

Bacterial glutamate transporters have aroused a lot of interest because the three-dimensional structure of the glutamate transporter Glt_{ph} from archaebacterium *Pyrococcus horikoshii* (*P. horikoshii*) was recently determined (Yernool *et al.*, 2004). In addition, because the overexpression of protein in bacteria results in much higher yields of protein, in comparison to eukaryotic cell expression systems (Kück, 2005), and the experimental success depends on the amount and purity of the produced protein, it is technically more feasible to study prokaryotic paralogs.

1.3.3 Stoichiometry

Glutamate transporters belong to the class of secondary active transporters that can use the potential energy of ion gradients to transport specific substrates against their concentration gradients. Glutamate transporters exhibit two fundamentally different transport mechanisms: the first is the coupled co-transport of substrate (glutamate or aspartate), with sodium, protons and potassium (Levy *et al.*, 1998; Zerangue *et al.*, 1996) and the second is a thermodynamically uncoupled, channel-like anion transport (anion channel function) (Fairman *et al.*, 1995; Wadiche *et al.*, 1995; Larsson *et al.*, 1996; Billups *et al.*, 1996; Melzer *et al.*, 2003). The exact molecular basis of these two diverse functions is not yet understood. The ion gradients of sodium and potassium ions and also protons deliver the driving force for glutamate uptake (Zerangue *et al.*, 1996).

EAAT2 and EAAT3 have been shown to exhibit the following stoichiometry: the co-transport of one glutamate molecule, three sodium ions and one proton into the cell is coupled to the counter-transport of one potassium ion out of the cell (Kanner *et al.*, 1978; Stallcup *et al.*, 1979; Schwartz *et al.*, 1990; Szatkowski *et al.*, 1990; Barbour *et al.*, 1991; Erecinska *et al.*, 1983; Zerangue *et al.*, 1996), see Fig. 1.5. It cannot be taken for granted that EAAT1, EAAT4, and EAAT5 share the same stoichiometry.

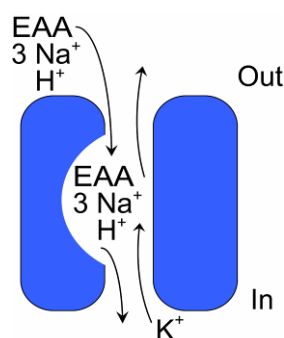


Figure 1.5 Stoichiometry of glutamate transporters. Coupled transport stoichiometry of mammalian glutamate transporters. One excitatory amino acid (EAA) molecule, three sodium ions (Na^+) and one proton (H^+) are co-transported into the cell and one potassium ion (K^+) is counter-transported outside.

Various EAATs paralogs have been identified in prokaryotes and shown to exhibit a variety of transport stoichiometries. Although these transporters have similar predicted structures, they exhibit distinct functional properties such as variations on a

common transport mechanism (Arriza *et al.*, 1994; Melzer *et al.*, 2003; Mim *et al.*, 2005). Whereas EAATs transport three sodium ions, one proton, and one glutamate molecule in counter-transport with one potassium ion, there are bacterial paralogs that only transport substrate (glutamate, aspartate) stoichiometrically coupled to protons, or to sodium. The glutamate transporters from *Escherichia coli* and from *Bacillus subtilis* use protons to drive glutamate uptake, and the glutamate transporter from *Escherichia coli* only depends on a proton gradient. The glutamate transporter from *Pyrococcus horikoshii* catalyzes aspartate transport solely coupled to sodium (Boudker *et al.*, 2007; Ryan *et al.*, 2009). A sodium / proton / L-glutamate symport has also been found for the glutamate transporters from *Bacillus stearothermophilus* and *Bacillus caldotenax* (Heyne *et al.*, 1991). However, these transporters lost their coupling sodium selectivity when they were expressed in *E. coli* (Tolner *et al.*, 1995a; Tolner *et al.*, 1995b).

Interest in bacterial glutamate transporters is high because there are indications that, by comparison, glutamate transport in eukaryotes is more complex and bacterial glutamate transporters exhibit less complicated transport processes, enabling more convenient analysis of the bacterial systems. In this work ecglTP, the glutamate transporter from *E. coli*, was used as a model protein to study the mechanisms underlying coupled glutamate transport.

1.3.4 Structure

Although they possess different functions, bacterial and mammalian glutamate transporters share strong homology to one another. Prokaryotic and eukaryotic glutamate and neutral amino acid transporters possess significant amino acid sequence homology throughout the entire primary structure, as revealed by multiple sequence alignments (Slotboom *et al.*, 1999).

Glutamate transporters are integral membrane proteins. Members of the glutamate transporter family share (1) similar transmembrane topology (Fig. 1.7) and (2) trimeric oligomerisation state (Gendreau *et al.*, 2004; Yernool *et al.*, 2004). ecglTP consists of 437 amino acids and a molecular mass of monomer is 47.2 kDa.

ecglTP has a typical amino acid composition for membrane proteins: 66.3 % of amino acids are non-polar and 32.7 % are polar, 6.9 % are basic and 6.4 % acidic. ecglTP shares 48 % sequence homology and 22 % identity with the human EAAT2

isoform. Glt_{ph} shares 37 % amino acid identity with human EAAT2. Glt_{ph} and ecgltP are 33 % identical and 55 % homologous in their primary sequences (Fig. 1.6, Fig. 1.7 B), (Table 7.2). A stretch of about 150 residues in the C-terminal half is particularly well conserved (Slotboom *et al.*, 1999). This half of the protein contains several sequence motifs involved in recognition and/or translocation of glutamate and co-transported cations (Slotboom *et al.*, 2001b).

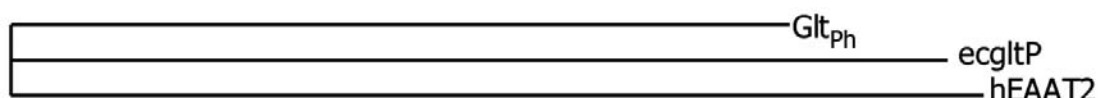


Figure 1.6 Phylogenetic relationship of three distantly related glutamate transporters Glt_{ph}, ecgltP, and hEAAT2. The phylogram is based on a multiple amino acid sequence alignment of respective sequences Glt_{ph} (Accession no. AB009510), ecgltP (Accession no. P21345), hEAAT2 (Accession no. P43004) (ClustalW, Chenna *et al.*, 2003). Abbreviations: glutamate transporter from archaeobacteria *P. horikoshii* (Glt_{ph}), bacterial glutamate transporter from *E. coli* (ecgltP), and human isoform of excitatory amino acid transporters (hEAAT2).

According to the crystal structure of the bacterial glutamate transporter Glt_{ph} from *Pyrococcus horikoshii*, the glutamate transporter is a bowl-shaped trimer (Fig. 1.8) with a solvent-filled extracellular basin extending halfway across the membrane bilayer. At the bottom of the basin are three independent binding sites, each cradled by two helical hairpins, facing opposite sides of the membrane. Transport of glutamate is thought to be mediated by movements of the hairpins that allow alternating access to either side of the membrane (Yernool *et al.*, 2004).

Glt_{ph} is a homotrimer, each subunit of which consists of eight transmembrane helices. Each protomer (Fig. 1.9) contains eight transmembrane segments, two re-entrant helical hairpins, and independent substrate translocation pathways. The first six transmembrane segments form a distorted “amino-terminal cylinder” and provide all interprotomer contacts, whereas transmembrane segments TM7 and TM8, together with hairpins HP1 and HP2, assemble to form a highly conserved core within the amino-terminal cylinder (Boudker *et al.*, 2007).

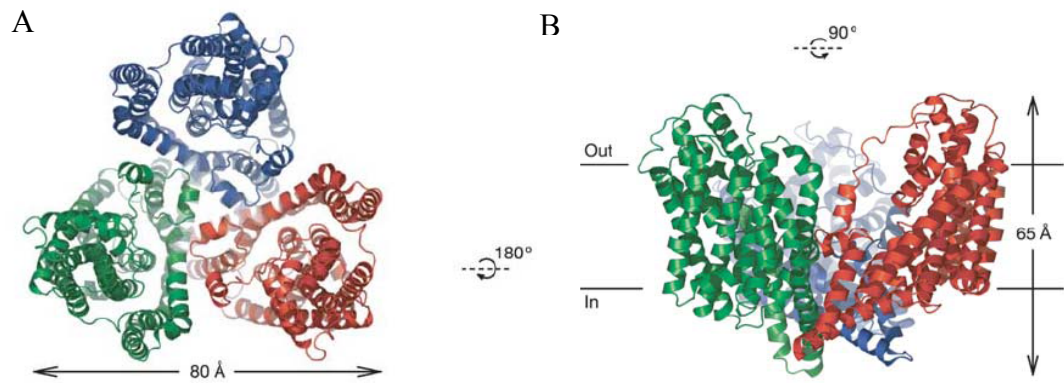


Figure 1.8 Crystal structure of a bacterial glutamate transporter Glt_{Ph} from *Pyrococcus horikoshii* (Yernool *et al.*, 2004). (A) Ribbon representation of the trimeric protein, in which the protomers are shown in red, blue and green, shown from the extracellular side of the plasma membrane. (B) View of the trimer parallel to the membrane.

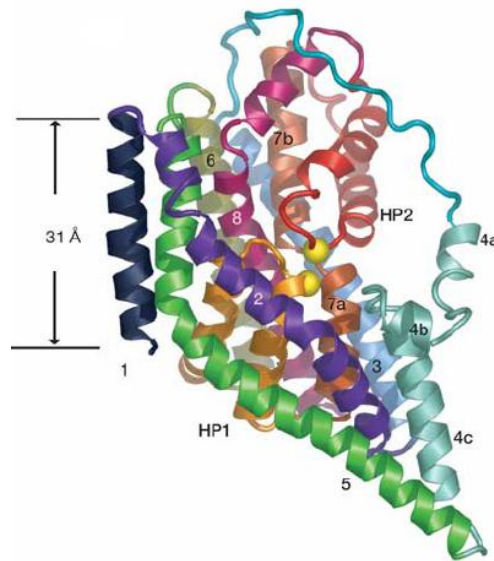


Figure 1.9 Protomer. Ribbon representation of the protomer viewed in the plane of the plasma membrane in which the transmembrane helices (1-8) and hairpins (HP1, HP2) are labelled and are shown in different colours (Yernool *et al.*, 2004).

The carboxy-terminal half of eukaryotic and prokaryotic transporters encompasses residues that are crucial for substrate binding, substrate transport and ion coupling (Kanner *et al.*, 2002; Yernool *et al.*, 2004 ; Boudker *et al.* 2007), whereas residues in the amino-terminal part are implicated in the thermodynamically uncoupled chloride flux (Ryan *et al.*, 2004).

Particularly, the arginine residue at position 447 was shown to play a role in determining substrate selectivity in EAAT3 (Bendahan *et al.*, 2000). The glutamate residue at position 373 was proposed to be the proton acceptor in EAAT3 (Greuer *et al.*, 2003). The same glutamate residue in GLT-1, the rat homolog of EAAT2 (E404), was proposed to bind K^+ (Kavanaugh *et al.*, 1997). Aspartate residues at position 367 of EAAT3 (Tao *et al.*, 2006; Tao *et al.*, 2007) and 405 of Glt_{ph} (Boudker *et al.*, 2007), were shown to be crucial for sodium binding.

1.4 Aim of the thesis

This study focuses on the molecular, biochemical and functional characterization of a model transport protein, the bacterial glutamate transporter from *Escherichia coli* – ecgltP – using the methods of mutagenesis, protein purification with subsequent reconstitution into artificial lipid vesicles, and quantification of radiotracer substrate fluxes into proteoliposomes. The possibility of studying a purified prokaryotic glutamate transporter protein using functional tests without contaminations with other cellular compartments gives, in combination with the available structural information, promising preconditions for the determination of transport mechanisms of glutamate transporters.

This project aims to characterize the functional properties of glutamate transporters in order to gain insights into the molecular mechanisms underlying coupled transport. To learn more about the structural basis of the transport properties of this prokaryotic glutamate transporter, the wild type ecgltP protein was characterized and compared with transporter carrying mutation, potentially affecting sodium binding (Fig. 1.10). N401D ecgltP contains an aspartate residue in TM8 at a position homologous to D405 of Glt_{Ph} (Boudker *et al.*, 2007), which was shown to be crucial for sodium binding.

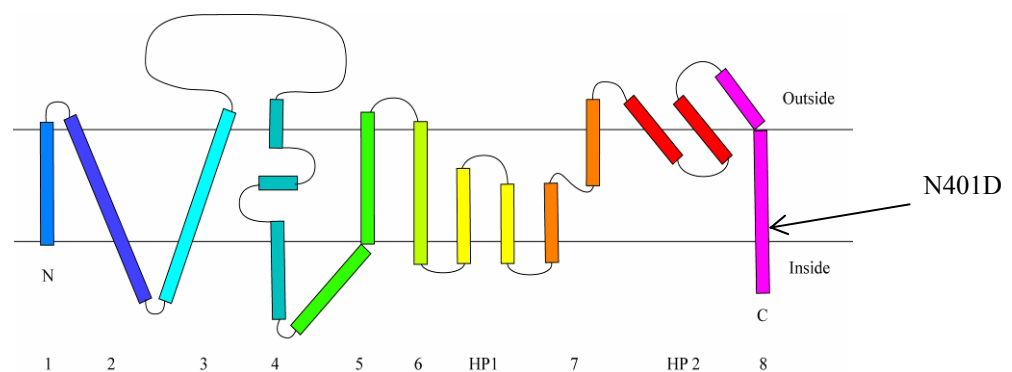


Figure 1.10 Localization of the N401D mutation. Schematic representation of ecgltP transmembrane topology showing the localization of mutated residue.

2. Materials and methods

2.1 Chemicals, materials and equipment

2.1.1 Materials and equipment

Equipment and materials were obtained from the following companies: Avestin Inc. (Ottawa, Canada), BD Microlance (USA), Beckman Coulter, Inc. (USA), Bio-Rad Laboratories GmbH (München, Germany), Biometra (Göttingen, Germany), Branson Ultrasonics Corp. (Danbury, USA), Corning (New York, USA), Eppendorf (Hamburg, Germany), GE Healthcare Bio-Sciences, formerly Amersham Biosciences (United Kingdom), Greiner Bio-One GmbH (Frickenhausen, Germany), G. Kisker GbR (Steinfurt, Germany), Hamilton Company (Nevada, USA), Heraeus (Newport Pagnell, United Kingdom), IBA (Göttingen, Germany), Ibidi GmbH (München, Germany), Infors HT AG (Bottmingen, Switzerland), Kimberley-Clarke (Roswell, USA), KNF Neuberger, Inc. (New Jersey, USA), Millipore Corporation (Billerica, USA), MJ Research, Inc. (Waltham, USA), PEQLAB Biotechnologie GMBH (Erlangen, Germany), PerkinElmer Life and Analytical Sciences (Rodgau, Germany), PTI (NJ, USA), QIAGEN GmbH (Hilden, Germany), Roth (Karlsruhe, Germany), Sartorius Biolab Products (Göttingen, Germany), Sarstedt (Nümbrecht, Germany), Schott Glaswerke AG (Mainz, Germany), Systat Software, Inc. (Point Richmond, VA, USA), Systec GmbH Labor-Systemtechnik (Wettenberg, Germany), VACUUBRAND GmbH (Wertheim, Germany), Whatman Laboratory Products, Inc. (Clifton, USA).

2.1.2 Chemicals

All chemicals and solutions had at least a purity grade of p.A. and were obtained from AppliChem GmbH (Darmstadt, Germany), ACROS ORGANICS (USA), Avanti Polar Lipids (Alabaster, AL, USA), JT Baker Chemical Co., (Phillipsburg, USA), Becton, Dickinson and Company (USA/France), Bio-Rad Laboratories GmbH (München, Germany), Calbiochem (Bad Soden, Germany), Carl Roth GmbH (Karlsruhe, Germany), Decon Laboratories Limited (East Sussex, United Kingdom), Fisher Scientific GmbH (Schwerte, Germany), Fluka (Neu-Ulm, Germany), GLYCON Biochemicals (Luckenwalde, Germany), Hartmann Analytic GmbH (Braunschweig, Germany), KMF Laborchemie Handels GmbH (Lohmar, Germany), Linde (Hannover, Germany), Merck KGaA (Darmstadt, Germany), MP Biomedicals, Inc. (Solon, USA), New England Biolabs GmbH (Frankfurt, Germany), PerkinElmer Life and Analytical

Sciences (Rodgau, Germany), Pierce (Rockford, USA), Serva GmbH (Heidelberg, Germany), Sigma-Aldrich (Hamburg, Germany), Stratagene (La Jolla, CA, USA), or USB Corporation (USA). Deionised water was prepared at 18.2 M Ω in a Milli Q plus system from Millipore (USA). For protein biochemical parts of the work, deionised and autoclaved water was also used.

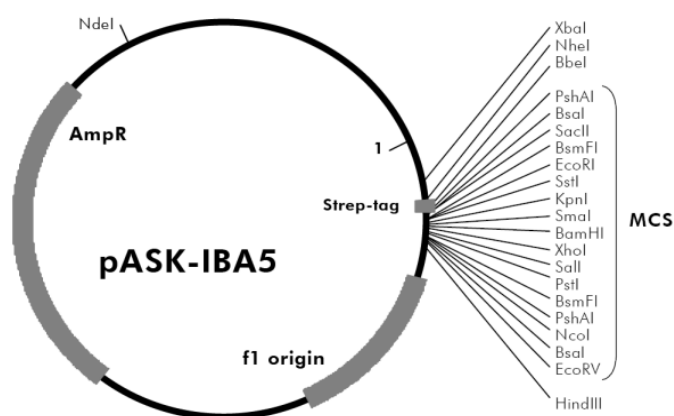
2.2 Molecular biology

2.2.1 Sequence alignments

Sequence alignments were made with use of Vector NTI Advance 10 software from Invitrogen (Invitrogen Corporation, CA, USA).

2.2.2 Plasmids

For ecgltP expression the vector pASK-IBA5 from IBA (IBA GmbH, Göttingen, Germany) was used. The cDNA encoding ecgltP was subcloned into the pASK IBA5 vector, which adds an amino-terminal Strep-tag (MASWSHPQFEK). This allows a



single step protein purification to purify the strep-ecgltP protein using *Strep-Tactin*[®] affinity chromatography (IBA). pASK IBA5 carries an ampicillin resistance cassette. The protein expression is under the control of Tet-promotors/operators, and can be induced by anhydrotetracycline hydrochloride.

2.2.3 Mutagenesis

2.2.3.1 Primers and resulting constructs

Table 7.5 shows the primers used for mutagenesis. Each primer was checked in Vector NTI Advance 10 (Invitrogen) for the presence of a low amount of predicted loops, one or more cytosine or guanine at both termini, a length of 25 to 45 bases, a

melting temperature of ≥ 78 °C, the mutation being in the middle of the primer and no or small negative dG (Gibb's free energy). A low dG value is associated with energetically stable interactions between palindromic sequences within primers and should therefore be avoided.

Constructs were made by polymerase chain reaction (PCR) using pASK-IBA5 ecglp as the template (2.2.3.2). The desired mutation was introduced by cleavage of the PCR product and the DNA fragment was then ligated into the previously mentioned vector. Mutation N401D ecglp was made with the Quikchange method (2.2.3.3) on pASK-IBA5 ecglp with the indicated primers. The sequencing primers were from MWG Biotech AG and the Quikchange primers from Sigma Aldrich. All DNA constructs were sequenced.

2.2.3.2 Polymerase Chain Reaction

The PCR is a technique based on the work of Mullis (Mullis *et al.*, 1990). Using PCR to generate multiple copies of a particular DNA sequence allows the amplification and qualitative analysis of DNA fragments. For analytical amplification and mutagenesis PCR the Taq-Polymerase (NEB, 5 U/mL) was used. 10-100 ng DNA-template were mixed with 10 μ M of each primer, 200 μ M dNTPs and 0.05 U/ μ L Taq-Polymerase in 1x PCR buffer. The reaction mixture was incubated in a thermocycler where, after denaturation at 94-96 °C for 1 minute, 35 cycles were performed.

Denaturation	1 min	94 °C
Annealing	1 min	40-72 °C (T_m -10 °C)
Synthesis	3 min	72 °C

Final synthesis took place at 72 °C for 10 min. The PCR product was purified using a QIAquick PCR Purification Kit or was electrophoresed on a 1 % agarose gel and then extracted from the gel using the QIAquick Gel Extraction Kit, to remove primers, nucleotides, salts and the DNA polymerase.

2.2.3.3 Quikchange method

Site-directed Quikchange mutagenesis was performed using a reaction mixture containing 50 ng of template DNA, 125 ng sense primer, 125 ng antisense primer, 2 % (v/v) 10 mM dNTP mixture (Eppendorf or Qiagen), and 10 % (v/v) 10x reaction buffer (Stratagene). The reaction was filled to a volume of 49 μ l with HPLC quality water before 1 μ l of Pfu Turbo DNA polymerase (2.5 U/ μ l, Stratagene) was added. The reaction was performed in a thermocycler, with a starting denaturation for 2 minutes at 95 °C followed by nineteen cycles.

Denaturing	45 sec	95 °C
Annealing	1 min	55 °C
Synthesis	1 min/kbp	68 °C

After these cycles the temperature was kept at 68 °C for 10 minutes more to allow the completion of the synthesis. The sample was then placed on ice for 2 minutes to cool the tube. 10 Units of DpnI (Fermentas or New England Biolabs) were added, which resulted in the selective digestion of the template DNA, leaving the mutated product intact, as DpnI only digests methylated DNA. Bacterial DNA is methylated, however the PCR synthesized DNA is not, as the appropriate enzymes are not present. The sample was incubated at 37 °C for 1 hour. Competent bacteria were transformed so that the target plasmid could be multiplied.

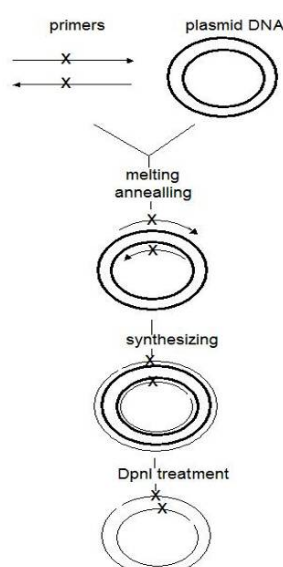


Figure 2.1 Scheme of the Quikchange reaction.

2.2.4 Transformation

Transformation of competent BL21 (DE3) and DH5 α *E. coli* cells was performed according to the method of Hanahan (Hanahan, 1983), with some modifications.

5 - 10 μ l of ligation mixture, respectively 10 to 50 ng DNA purified plasmid DNA was added to 40 μ l of competent *Escherichia coli* bacteria. After thawing the bacteria, the DNA was added and the mixture was incubated on ice for 20 minutes. The tube was transferred to a heat block for 60 seconds at 42 °C and then placed on ice for 2 minutes. After the addition of 300 μ l of LB medium, the bacteria were incubated at 37°C for 1 hour, shaking at 220 rpm. The bacteria were spun down for 0.5 minutes at 6,000 rpm, in a table centrifuge. The pellet was resuspended in a small part of the supernatant which was then transferred to an agar plate with the appropriate antibiotics (typically ampicillin, 0.05 mg/ml) to select for the desired plasmid. The plates were inverted to avoid the accumulation of condensed water on the colonies, and incubated overnight at 37 °C. For each transformation ligation mixture, a vector alone, a positive (50 ng of a high copy plasmid with the same antibiotics resistance) and negative (autoclaved deionised water or nothing instead of DNA) controls were used.

2.2.5 Plasmid recovery / purification / storage

Small amounts of DNA were recovered from 6 to 8 ml overnight cultures, grown at 37 °C and shaken at 220 rpm, in LB medium with the appropriate antibiotics. According to the protocols of the Qiaprep 8 Miniprep Kit, or Qiaprep Spin Miniprep Kit with the use a vacuum pump or table centrifuge as applicable, the plasmids were isolated. Larger quantities of DNA were recovered/purified with the Qiagen HiSpeed Plasmid Maxi Kit. As preparation, 2 ml of LB medium with the appropriate antibiotics were inoculated with transformed *E. coli* as preculture, which grew at 37 °C for 8 hours. The preculture was given into 200 ml LB medium with the appropriate antibiotics. This culture was incubated overnight at 37 °C, shaking at 220 rpm. All steps were followed as recommended by the manufacturer. For storage, 1 ml of the grown culture was taken. The same volume of 50 % glycerol was added before the mix was flash frozen in liquid nitrogen. Afterwards these glycerol stocks were kept at -80 °C until used.

2.2.6 DNA concentration measurement

DNA concentrations were measured after dilution 1:100 in autoclaved deionised water. The optical density (OD) was measured at 260 nm and 320 nm (baseline) in a spectrophotometer that automatically calculates the DNA concentration, or the DNA concentration was calculated manually. An OD₂₆₀ of 1 represents 50 µg/µl of DNA. The following formula was used for the manual calculation:

$$c(\text{dsDNA}) = \Delta A(260 \text{ nm} - 320 \text{ nm}) \cdot 50 \text{ µg/ml.}$$

2.2.7 Agarose gel electrophoresis

Agarose was dissolved in 1x TAE buffer (50x consists of 2 M Tris Base, 5.95 % (v/v) of 96 % Acetic acid, 10 % (v/v) 0.5 M EDTA, pH 8.0 or 3.72 % (w/v) Na₂EDTA · 2 H₂O), at a concentration dependent on the size of the DNA fragments to be analysed. The agarose concentrations used were 1 % (w/v) for fragments smaller than 1000 basepairs (bp) and 2 % (w/v) for fragments bigger than 1000 bp. Ethidium bromide was dissolved in the agarose gels at 0.002 % (v/v) at approximately 60°C. Ethidium bromide is an intercalating agent that fluoresces when exposed to UV-light, allowing the visualisation of DNA. The lambda DNA/EcoRI+HindIII marker or the GeneRuler DNA Ladder Mix was also loaded on the gel to provide a guide to the sizes of the DNA fragments. Samples were dissolved in 6x loading buffer (0.25 % bromophenol blue, 0.25 % xylene cyanol FF, 30-40 % glycerol). Gels were run at 100 V for 1-2 hours, DNA-visualisation via a Gel Doc™XR documentation system took place and bands were then quantified using the Quantify One program (BioRad) under UV light (with a wavelength of 302 nm). Plasmid DNA was isolated from preparative agarose gels using the QIAquick Gel Extraction Kit from Qiagen according to the manufacturer's instructions.

2.2.8 DNA Restriction Enzymes

For fragments up to 3000 bp in length, 5 µg and for bigger fragments 3 µg of DNA was used. The appropriate amount of DNA was used together with 10 % (v/v) 10x enzyme buffer, 1 % (v/v) BSA or SAM if required, the reaction was filled to a volume

of 48.5 μl with autoclaved deionised H_2O and 1.5 μl of enzyme (New England Biolabs) was used. For a double digest with compatible buffers the reaction was filled to 47 μl and 1.5 μl of each of the two enzymes were added. When the buffers of the different enzymes were not compatible, but differed only in salt concentration, one digest was performed for 2 hours after which NaCl and the second enzyme could be added. If there were other differences between the two buffers to be used, the digested DNA was PCR purified using the Qiaquick PCR Purification Kit or electrophoresed on an agarose gel and then extracted from the gel. After these purification steps the DNA was then digested with the second enzyme in the appropriate buffer. Test restrictions were performed in a total reaction volume of 20 μl , of which 10 % (v/v) was DNA and 5 % (v/v) was enzyme. Restriction enzymes were applied in concentrations of from 2 to 10U per reaction mix. In preparative reactions from 500 ng to 2 μg DNA was used, and for analytical reactions 2-5 μl of miniprep-DNA was used.

2.2.9 Gel extraction

DNA was extracted from agarose gels by a QIAquick Gel Extraction Kit according to the manufacturer's instructions. Alternatively, DNA fragments larger than 1000 bp were purified with glass milk. The DNA fragment was cut out of the agarose gel and weighed. For the glass milk purification the gel was dissolved in 3 volumes of filtered sodium iodide solution (6 M NaI, 10 mM Na_2SO_3 , and 20 mM Tris HCl) at 65°C for at least 5 minutes. The mixture was cooled and then mixed with 10 μl vortexed glass milk. The mixture was vortexed several times during 10 minutes of incubation at room temperature. Centrifugation at 5,900 g for 10 seconds in a table centrifuge pelleted the glassmilk. The pellet was washed with 600 μl NEET wash solution (100 mM NaCl, 1 mM EDTA, 50 % ethanol, 10 mM Tris HCl, pH 7.5), by vortexing and centrifugation. The pellet was washed again with 400 μl NEET wash solution and after removal of the supernatant it was additionally centrifuged at 16,100 g. The supernatant was completely removed and the glass milk was dried for 10 minutes of centrifugation at 30 °C under vacuum in a concentrator (vacuum concentrator 5301 from Eppendorf). The DNA was eluted from the glass milk by addition of 30 μl elution buffer from Qiagen and incubation for 10 minutes at 65 °C. Centrifugation for 30 seconds at 16,100 g was needed to obtain the supernatant. The centrifugation step was repeated to ensure that there was no glassmilk left in the DNA fraction.

2.2.9.1 Glass milk preparation

50 g of silica was stirred for 1 hour in 200-300 ml of deionised water. After 2 min without stirring the supernatant was transferred to a beaker and left to stand for another minute. The supernatant was discarded and the pellet was centrifuged for 5 minutes at 1,200 g. The pellet was resuspended in 100 ml 50 % HNO₃ and was boiled for 1 hour under a hood. After cooling down and centrifugation as before, the silica was washed 4 to 6 times with deionised water until the pH was 7.0. The pellet was resuspended in an equal volume of deionised water to form a 50 % suspension and was frozen at -20 °C in 0.5 ml aliquots.

2.2.10 Ligation

Restriction fragments were separated on a 1 % agarose gel and were visualised with the Gel-Documentation system, using the Quantify One program to quantify the bands. Ligations were composed of a ratio of 1:3 of the biggest plasmid fragment to the inserted fragments, 2 µl T4 DNA ligase buffer, autoclaved deionised H₂O to a final volume of 19 µl and 1 µl T4 DNA ligase (Fermentas). Ligation took place for 2 hours at room temperature or 24 hours at 4 °C. After the ligation reaction was complete the bacteria were transformed with the reaction mixture.

2.2.11 DNA sequencing

250 ng of DNA, dissolved in HPLC quality water, was used. To the DNA 10pmol of sense or antisense primer was added, 2 to 4 µl premix (Big Dye Terminator v1.1 Cycle Sequencing Kit from Applied Biosystems) and HPLC quality water to a total reaction volume of 10 µl. The sequencing PCR took place in a thermocycler with a heated lid for 25 cycles.

Denaturation	30 sec	96 °C
Annealing	20 sec	45-52 °C (T _m 5 to 10)
Synthesis	4 min	60 °C

DNA was purified with a DyeEx 2.0 Spin Kit from Qiagen or by ethanol precipitation. DNA was placed at 90 °C for 2 minutes for denaturing and then was incubated for 5 minutes on ice after which the reaction was transferred to a PCR sequencing facility (Department of Microbiology of the Hannover Medical School) where DNA sequence was analysed using the Genetic Analyser 3130 XL system from Applied Biosystems.

2.2.11.1 Ethanol precipitation of sequenced DNA

Sequencing mixture $x \mu\text{l}$ was placed in a 0.5 ml tube and was subsequently mixed with a mixture of 90 μl HPLC quality water and $0.1 \cdot x \mu\text{l}$ 3 M sodium acetate pH 5.2 and then with $2.5 \cdot x \mu\text{l}$ 100 % ethanol (stored at $-20 \text{ }^\circ\text{C}$), and incubated for 10 minutes at $-20 \text{ }^\circ\text{C}$. The mixture was then centrifuged for 20 minutes at 14,000 g after which the ethanol was removed. The pellet was washed with 250 μl 70 % ethanol and centrifuged for 7 minutes at 16,100 g. The supernatant was removed and the pellet was dried for 5 minutes at 30 °C under vacuum. The pellet was dissolved in $2.5 \cdot x \mu\text{l}$ of HPLC quality water.

2.2.12 LB medium, agar plates and antibiotics

LB medium was made by dissolving 22.5 g Difco™ LB Broth, Miller (Luria-Bertani) in deionised water to a final volume of 900 ml. After dissolving, the solution was autoclaved immediately. For agar plates 22.5 g Difco™ LB Broth, Miller (Luria-Bertani) and 18 g of Bacto™ Agar were dissolved to a total volume of 900 ml in deionised water, stirred and autoclaved. After cooling down to 50 °C the appropriate antibiotic was added to the flask to give a final 1x solution. Plates were poured under a clean bench and stored dry at 4 °C. In most cases, ampicillin was added. The ampicillin stock solution was prepared by dissolving ampicillin powder in autoclaved deionised water. A 1000x ampicillin stock solution contained 100 mg ml⁻¹ (150 $\mu\text{g}/\text{ml}$), and was aliquoted. Aliquots were stored at $-20 \text{ }^\circ\text{C}$.

2.2.13 Competent bacteria

For the production of the chemically competent *E. coli* bacteria, *E. coli* BL21 (DE3) or *E. coli* DH5 α bacteria were added to 5 ml of LB medium and incubated

overnight at 37 °C, shaking at 250 rpm. 0.4 ml of this culture was diluted in 40 ml LB media and this culture of *E. coli* was grown to its exponential phase at an OD₆₀₀ of 0.3-0.5. Bacteria were harvested at 4 °C, 3,000 g for 10 min and were kept on ice from then on. The pellet was resuspended in 30 ml TFB I (100 mM RbCl, 50 mM MnCl₂ · 2 H₂O, 30 mM potassium acetate, 10 mM CaCl₂ · 2 H₂O, 15 % (v/v) glycerol, pH 5.8) and was incubated for 20 to 90 min on ice. Bacteria were harvested again at 3,000 g at 4 °C for 10 minutes and were resuspended in 3 ml TFB II (10 mM MOPS, 10 mM RbCl, 75 mM CaCl₂ · 2 H₂O, 15 % (v/v) glycerol, pH 8.0). These competent bacteria were aliquoted, immediately frozen in liquid nitrogen and stored at -80°C.

2.3 Protein biochemistry

The protocol for the purification of ecgltP is based on the purification protocol for CIC channels (Maduke *et al.*, 1999) and has been optimized in our laboratory.

2.3.1 Expression of ecgltP

As a pre-culture for induction, 70 ml LB media in a 250 ml flask was inoculated with *E. coli* BL21 (DE3) or DH5α bacteria cells containing the pASK IBA5-ecgltP plasmid, from a glycerol stock. Two flasks of medium were always inoculated to produce a sufficient volume of the culture to express the protein on the following day. 70 µl of 100 mg/ml ampicillin stock in H₂O was added to each flask. The following incubation was performed overnight at 37 °C, shaking at 250 rpm.

The pre-culture was diluted 1:50 and grown in 450 ml LB media at 37 °C, shaking at 250 rpm until an OD₆₀₀ of 0.6-0.7, was reached. After this protein expression was induced with 200 µg/l anhydrotetracycline hydrochloride (AHT) for the next three hours at 37 °C, and the bacteria were then harvested by centrifugation at 5,000 g at 4°C. At appropriate stages, before and after induction samples for SDS-PAGE (sodiumdodecylsulfat polyacrylamide gel electrophoresis) analysis were taken (see 3.1). Bacteria pellets were immediately flash frozen in liquid nitrogen and stored at -80 °C until used.

2.3.2 *Bacteria lysis and membrane pellet preparation*

The bacteria pellet (corresponding to 450 ml culture) was thawed on ice for 5-10 min and resuspended immediately in 40 ml pre-chilled buffer W (100 mM Tris-HCl, 150 mM NaCl, 1 mM EDTA, pH 8.0). Protease inhibitors were added before bacteria lysis by sonication: 1 µg/ml pepstatin, 10 mM β-mercaptoethanol, 1 µg/ml leupeptin, 1 mM PMSF. Sonication was performed on ice for 6 × 20 sec at 40 % power using an ultrasound sonifier 450 (Branson Ultrasonics Corp.), while the metal beaker was rotated, with a 20 sec pause in between the pulses. The next centrifugation step was done immediately at 4 °C in pre-chilled flasks at 12,000 g-15,000 g for 20 min. The supernatant was saved and transferred to pre-chilled ultracentrifuge tubes and ultracentrifuged for 60 min at 110,000 g at 4 °C to separate the membrane fraction. Each pellet was resuspended in 4 ml buffer W supplemented with 250mM sucrose and diluted to OD₂₈₀ = 20. At appropriate stages samples for SDS-PAGE analysis were taken (see 3.1). The membrane fraction pellets were aliquoted and immediately flash frozen in liquid nitrogen and stored at -80 °C until used.

2.3.3 *Solubilization of ecgltP from the membrane pellet*

The frozen membrane pellet was thawed on ice. After solubilization of the membrane fraction with 15 mM n-Dodecyl-β-maltoside (DDM) for two hours, stirring at 4 °C, the solubilization mix was ultracentrifuged for 60 min at 110,000 g at 4 °C. The supernatant, containing soluble strep-ecgltP, was retained for further use. To assess solubilisation the pellet was resuspended in urea buffer (100 mM NaH₂PO₄, 10 mM Tris-HCl, 8 mM urea, pH 8.0) to the original volume, a sample for the SDS-PAGE was taken (see 3.1) and the rest was discarded.

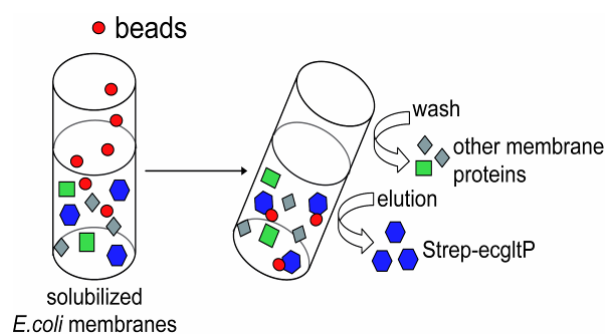
2.3.4 *Purification of ecgltP by affinity chromatography*

ecgltP was purified in one step by affinity chromatography using a Strep-Tactin[®] Superflow[®] High Pressure column and the ÄKTAprime[™]plus system (from GE Healthcare Bio-Sciences) according to the manufacturer's instruction manual. All reagents, solutions, columns and beakers were pre-cooled to the running temperature (4-6 °C) in chromatography cabinet. The column was stored in buffer R (1 mM HABA in

buffer W), giving a red color to the resin. The column was washed twice with 5x column volume (CV) of buffer W. Equilibration of the column was performed with 4x CV with buffer W supplemented with 1 mM DDM. The supernatant containing the solubilized ecgltP protein was diluted 3 to 5 times in buffer W without DDM, to a final DDM concentration 3-5 mM.

After this the protein sample was applied to the column. The column was washed with 5x CV of 1 mM DDM in buffer W until the baseline absorbance measured by the UV detector at 280 nm was reached, to ensure that all unbound proteins were removed. The buffer was

then changed to the elution buffer E (2.5mM desthiobiotin in buffer W containing 1 mM DDM) for the following elution. The eluted protein was collected using the fraction collector, with a fraction volume equal to half of the CV. Protein was typically eluted in the 4th to 8th fractions. At appropriate stages, a sample for SDS-PAGE analysis was taken (see Fig. 3.1).



2.3.5 Size-exclusion chromatography

Purified ecgltP subjected to size-exclusion chromatography (SEC), also called gel-filtration or gel-permeation chromatography (GPC). SEC separates molecules of different sizes using porous matrix. It is generally used to separate biological molecules, and to determine molecular weights and molecular weight distributions of polymers, especially for proteins. Molecules larger than the larger pore size of the matrix can not enter the pores and elute in the void volume (V_0). Molecules that can enter the pores will have an average residence time that depends on the molecule's size and shape. Different molecules therefore have different total transit times through the column. Molecules that are smaller than the pore size can enter all pores, and have the longest residence time on the column and elute later. The ecgltP sample was loaded to the Superdex 200 10/30 column, connected to fast protein liquid chromatography (FPLC) or to automatic ÄKTAprime™plus system, running buffer was buffer W, containing 1 mM DDM. Applying 1 mM DDM detergent conserved the native trimeric (141.6 kDa) subunit of ecgltP (Gendreau *et al.*, 2004).

2.3.6 SDS-PAGE analysis

SDS-PAGE gel electrophoresis was performed using 12 % gels. Table 2.1 shows the constituents of the different solutions used for these gels. APS was prepared freshly as a 10 % solution in deionised H₂O. The polymerisation of the running gel was allowed to proceed for about 30 minutes. After this the 3% stacking gel was poured. Gels were run in running buffer (25 mM Trisbase, 192 mM glycine and 3.5 mM SDS, pH 8.3), first at 100 V and when samples had entered the separation gel the voltage was increased to 180 V.

Table 2.1 Constituents of the running and stacking gels of SDS gels. Protogel is an acrylamide-bisacrylamide 37.5:1 mixture (Serva).

Stock solution	Running gel, 12 %	Stock solution	Stacking gel, 3 %
40 % Protogel	4 ml	7.5 % Protogel	650 µl
1.5 M Tris, pH 8.8	2.5 ml	125 mM Tris-HCl, pH 6.8	1.2 ml
10 % SDS	100 µl	10 % SDS	50 µl
0.1 g/ml APS	100 µl	0.1 g/ml APS	25 µl
TEMED	10 µl	TEMED	5 µl

SDS loading buffer (2x): 125 mM TrisHCl, 4.1 % SDS, 20 % glycerol, 200 mM DTT, 0.014 mM bromphenol blue.

2.4 Functional assays

For functional tests *ecgltP* protein was reconstituted into artificial liposomes and transport was determined by measuring the accumulated radioactively labeled substrate inside the proteoliposome.

2.4.1 *ecgltP* reconstitution protocol

Reconstitution was performed essentially as described by Knol (Knol *et al.*, 1996). Liposomes were prepared from a n-pentane washed mixture of *E. coli* total Lipid Extract and L- α -phosphatidylcholine in 3:1 molar ratio in chloroform, dried under nitrogen and finally by vacuum to remove the chloroform. Lipids were resuspended in

buffer (50 mM KH_2PO_4 , pH 7.0) to a final concentration of 20 mg of lipid per milliliter. The suspension was frozen in liquid nitrogen, thawed slowly and extruded through a 400 nm polycarbonate membrane filter (Mayer *et al.*, 1986) using Membrane Extruder for Laboratory (from Avestin Inc.). The liposomes thus obtained were diluted 6-fold in the same buffer and treated with increasing amounts of 10 % Triton X-100. The solubilization of the liposomes with Triton X-100 was followed by measuring the optical density at 540 nm (Rigaud *et al.*, 1995) and the purified ecgltP was added (Fig. 2.2).

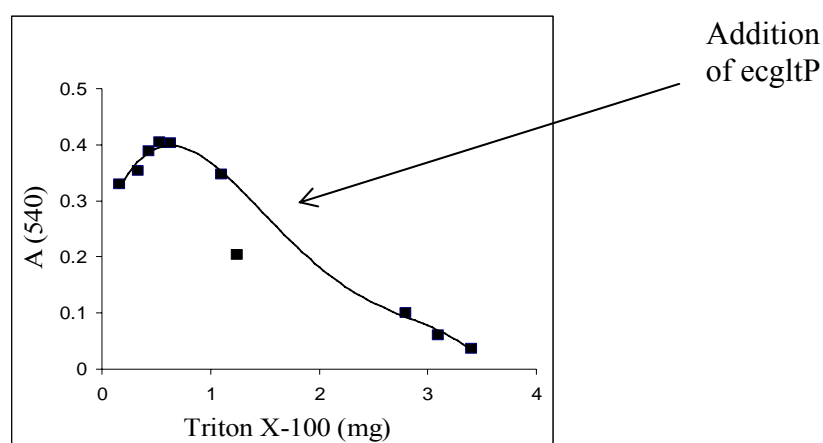


Figure 2.2 Solubilization of liposomes. Treatment of the liposome solution with increasing amounts of 10 % Triton X-100. The optical density was monitored at 540 nm.

Unless otherwise stated, a protein/lipid ratio of 15 $\mu\text{g}/\text{mg}$ was used. After addition of the purified protein, the mixture was rotated first at room temperature for 30 minutes, after which proteoliposomes were formed by removal of the detergent by three successive extractions with Bio-Beads SM-2 AdsorbentTM polystyrene beads. The first extraction was performed at room temperature for 2 hours, and the second and third were at 4 °C for 2 hours and 16 hours, respectively. The beads were removed by filtration over glass wool, and the proteoliposomes were recovered by ultracentrifugation at 100,000 g for 30 minutes. The proteoliposomes were resuspended in the appropriate buffer and flash frozen in liquid nitrogen and stored at -80 °C until used.

2.4.2 L-[³H]-glutamate / L-[³H]-aspartate uptake

Assays of L-[³H]-glutamate / L-[³H]-aspartate uptake driven by artificial gradients were performed essentially as described by Konings group (Tolner *et al.*,

1995b). For uptake experiments, to ensure a homogenous distribution of vesicle size, vesicles were frozen, thawed and subsequently extruded through the 400 nm polycarbonate membrane filter. Unless otherwise stated, the proteoliposomes were resuspended in buffer A (20 mM MES, 100 mM potassium acetate, 5 mM MgSO₄, pH 6.0). Uptake was measured at 22 °C. If necessary, temperatures were modified (Fig. 3.15) by incubation in the Thermostat Plus system (Eppendorf).

L-[³H]-glutamate / L-[³H]-aspartate uptake was initiated by diluting 25 µl of the proteoliposomes in 650 µl of buffer B (unless otherwise stated buffer B contains 120mM MES, 100 mM NaOH, 5 mM MgSO₄, and 0.0175 µM L-[³H]-glutamate or 0.0175 µM L-[³H]-aspartate, pH 6.0). After the specified incubation periods, the samples were diluted in 1 ml of ice-cold stop solution (100 mM LiCl, 100 mM HEPES, pH 8.0) followed by immediate filtration over cellulose nitrate filters (pore size 0.45 µm) from Sartorius. Filters were washed with an additional 3 ml of stop solution and were assayed for the presence of radioactivity and then measured using a liquid scintillation counter (TRICARB 2800 TR). Vesicles without protein were used in control experiments.

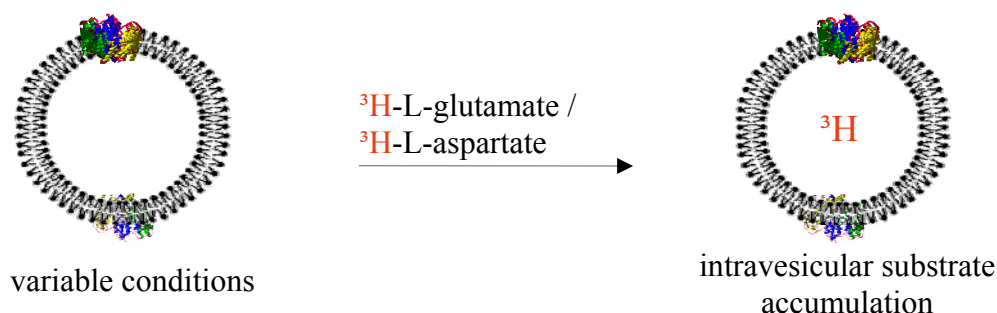


Figure 2.3 Schematic demonstrations of eglTP reconstitution in lipid vesicles and the uptake experiment.

To study the underlying transport mechanism, the intra- and extravesicular ionic composition was modified. In all experiments, the intravesicular buffering capacity was increased by equimolar substitution of acetate with HEPES. Buffers A and B were modified to study glutamate transport at different ionic conditions, and for clarity the conditions of each experiment are also shown schematically in the respective figures. The intravesicular solution was modified by several rounds of ultracentrifugation (100,000 g for 30 minutes), and resuspension of the proteoliposomes in solutions with differing composition and extrusion through a 400 nm polycarbonate membrane filter. [Na⁺] and [K⁺] concentrations were modified by equimolar substitution with NMDG. The pH was adjusted by replacing MES with the appropriate buffer hydroxides of the

major cations. In some of the experiments, intravesicular acetate was replaced with AMPSO, HEPES, or MES in order to increase the buffering capacity of the intravesicular solution.

In the majority of experiments, to study the underlying transport mechanism the membrane potential of vesicle was modified by the addition of valinomycin to the vesicle suspension at a concentration of 2.5 μM , either in order to hyperpolarize the vesicles or to clamp their membrane potential to 0 mV. For static head experiments (Fukuhara *et al.*, 1984; Turner, 1985) (Fig. 3.12), proteoliposomes were loaded with L-[^3H]-glutamate by incubation with 0.34 μM L-[^3H]-glutamate at intra- and extravesicular 120 mM MES, 100 mM KOH, 5 mM MgSO_4 , 2.5 μM valinomycin, pH 7.0 until reaching steady-state values. Control vesicles were formed in the same medium, containing 0.34 μM L-[^3H]-glutamate, by repeated freezing, thawing, and final sonicating. The experiment was initiated by diluting the vesicles 1:9 in modified buffer B with pHs of 5.0, 6.0, 6.75, and 6.8, supplemented with 2.5 μM valinomycin.

2.4.3 Data analysis

Nonlinear regression fits of experimental and calculated data were performed using SigmaPlot (Systat Software, Inc). Each figure either shows means \pm SEM from at least four samples of at least two separate experiments or a representative experiment that was performed at least four times. In each graph, data generated using at least two different proteoliposome preparations under different uptake conditions were compared. Transport rates were determined as inverse time constants from a fit of the time course of radioactive glutamate accumulation inside the vesicle with a monoexponential function. The time constants were then converted into transport rates given as the number of glutamate molecules transported per second using the L-[^3H]-glutamate calibration curve of scintillation counter. Dividing this value by the number of ecglTP monomers obtained from Bradford analysis resulted in unitary transport rates. Temperature coefficients (Q_{10}) and apparent activation energies (E_A) were extracted from individual transport rates using the Arrhenius equation:

$$v(T) = Ae^{-E_A/RT}$$

where v is the initial transport rate at 0 s, T the temperature, R the gas constant, and A the constant factor. The Q_{10} was calculated from E_A according to:

$$Q_{10} = v(T+10K)/v(T) \text{ for } T = 283$$

3. Results

3.1 ecglTP protein purification

ecglTP was cloned and overexpressed in *E. coli*. The membrane fraction was isolated from bacteria and purification was performed by one affinity chromatography step (Fig. 3.3 A). This resulted in a pure and homogenous population of trimeric ecglTP as shown by the results of size-exclusion chromatography (Fig. 3.3 B) and SDS PAGE analysis (Fig. 3.1, Fig. 3.2).

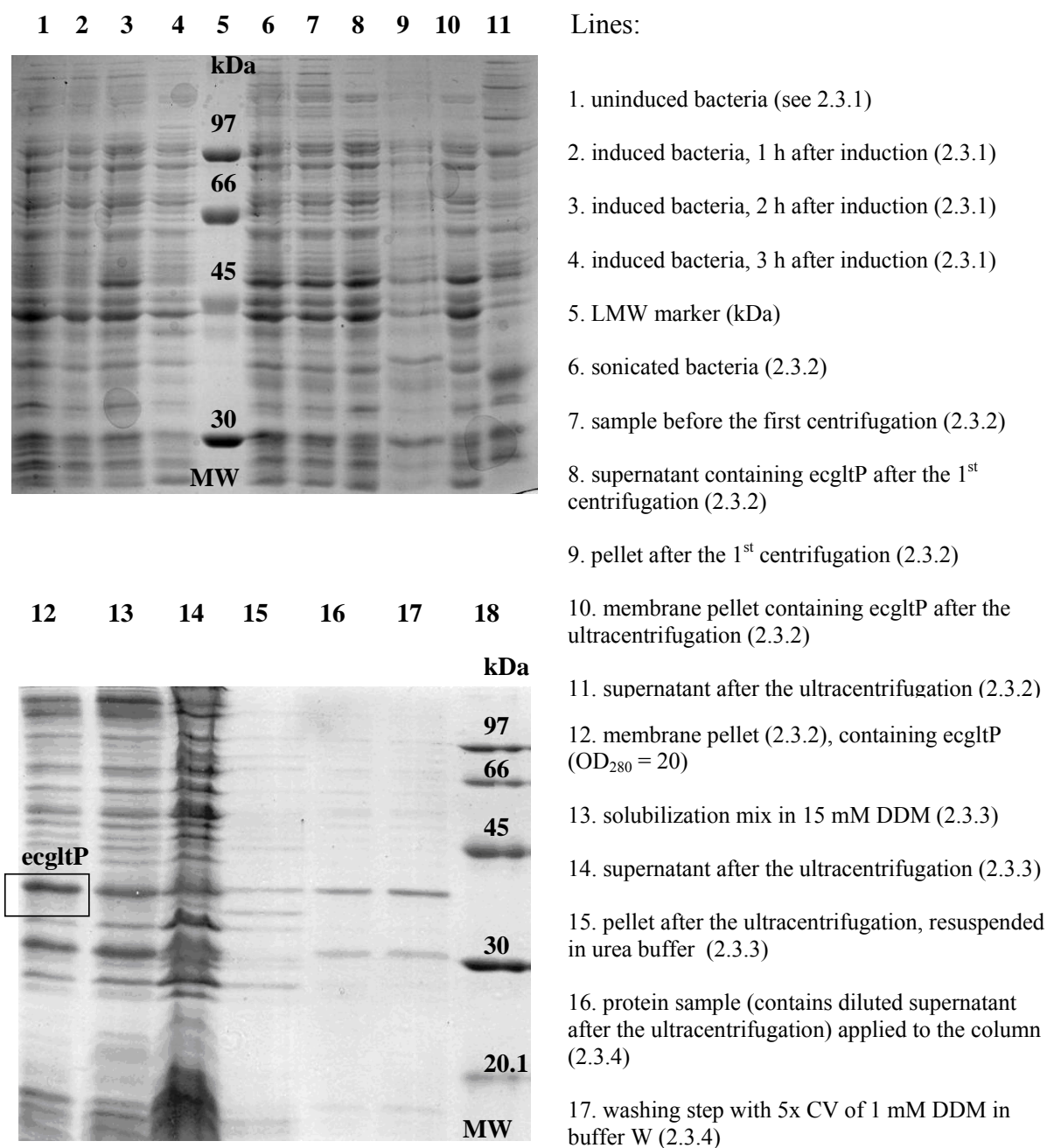


Figure 3.1 Overexpression and purification of ecglTP. Coomassie staining of a 12 % SDS-PAGE gel. Lanes 5 and 18: molecular mass standard LMW (low molecular weight marker from GE Healthcare) is shown with the molecular weight in kDa. MW, molecular weight.

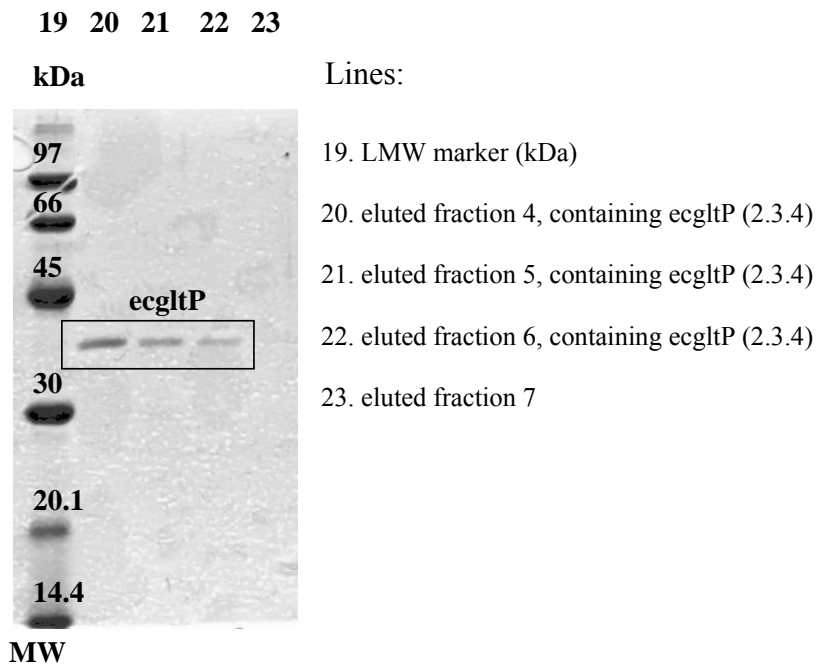


Figure 3.2 Purified ecgltP. Coomassie staining of a 12 % SDS-PAGE gel of strep-tagged ecgltP purified from *E. coli*. Lane 19: molecular mass standard LMW (low molecular weight marker from GE Healthcare) is shown with the molecular weights indicated in kDa. MW, molecular weight. A protein band can be seen at approximately 40 kDa, corresponding to monomeric ecgltP (Gendreau *et al.*, 2004).

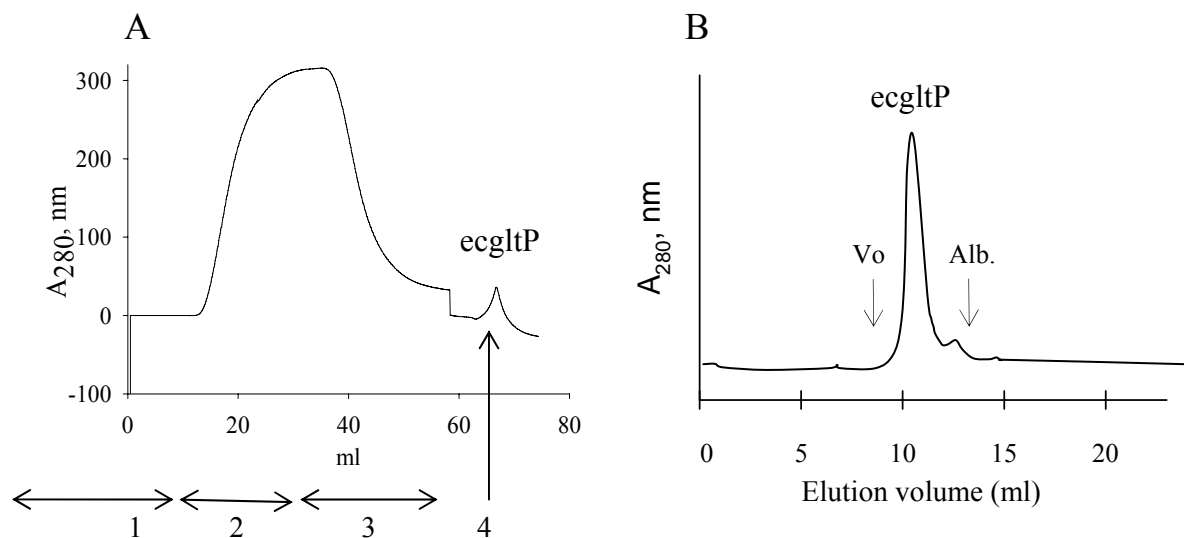


Figure 3.3 Affinity and size-exclusion chromatography elution profiles of ecgltP. (A) Monitoring at 280 nm of different steps of the strep-tagged affinity chromatography purification using a Strep-Tactin[®] Superflow[®] High Pressure column: (1) equilibration of the column, (2) loading of the protein containing sample, (3) washing step and (4) elution of the ecgltP protein. (B) Elution profile monitored at 280 nm from size exclusion chromatography using a Superdex 200 column (24-ml bed volume). *V_o*, void volume, *Alb.*, the elution volume of albumin (67 kDa). (A, B) Both columns were equilibrated with 1 mM DDM in Buffer W: 100 mM Tris-HCl, 150 mM NaCl, 1 mM EDTA, pH 8.0.

3.2 Purified and reconstituted ecgltP mediates substrate transport into proteoliposomes

3.2.1 Glutamate accumulation by proteoliposomes containing purified ecgltP

The time course of radioactive glutamate accumulation by proteoliposomes containing purified ecgltP in standard intravesicular and extravesicular solutions (see 2.4.2) is shown in figure 3.4. At $t = 0$ min, the radioactive sample was applied and proteoliposomes containing ecgltP accumulated glutamate, reaching a steady state after 40 min. A control experiment was carried out in parallel using vesicles without the ecgltP protein. Uptake into the control vesicles was negligible. Thus, reconstitution resulted in assembly of functional ecgltP in the artificial vesicular membranes.

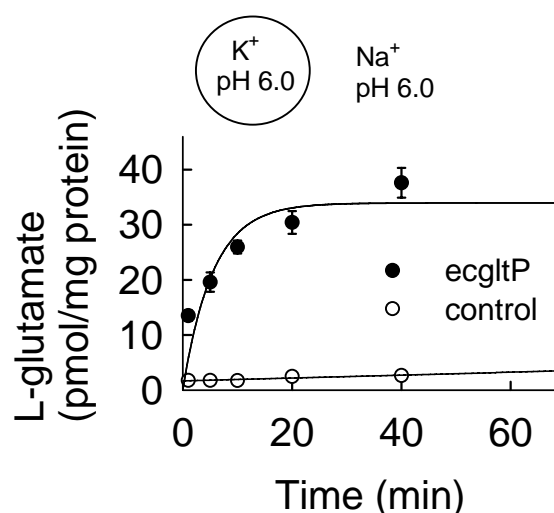


Figure 3.4 Purified and reconstituted ecgltP mediates glutamate transport into liposomes. Time course (solid lines give fits to these time dependences with monoexponential functions) of L-[³H]-glutamate accumulation in ecgltP-containing vesicles (●, $n = 4$) or control vesicles without protein (○, $n \geq 4$) at symmetrical potassium concentrations, pH_o 6.0 and pH_i 8.0, in the presence of valinomycin.

The transport rates rise in a linear fashion dependent on the amount of reconstituted ecgltP present, from 2 to 10 $\mu\text{g}/\text{mg}$ lipid (Fig. 3.5), indicating complete reconstitution of functional transporter in this range of protein/lipid ratios. Increased protein/lipid ratios result in larger percentages of vesicles containing at least one functional transporter and therefore an increased fraction of vesicles capable of accumulating L-[³H]-glutamate. This data indicate, that vesicular L-[³H]-glutamate accumulation is a specific result of glutamate transport by purified and reconstituted ecgltP.

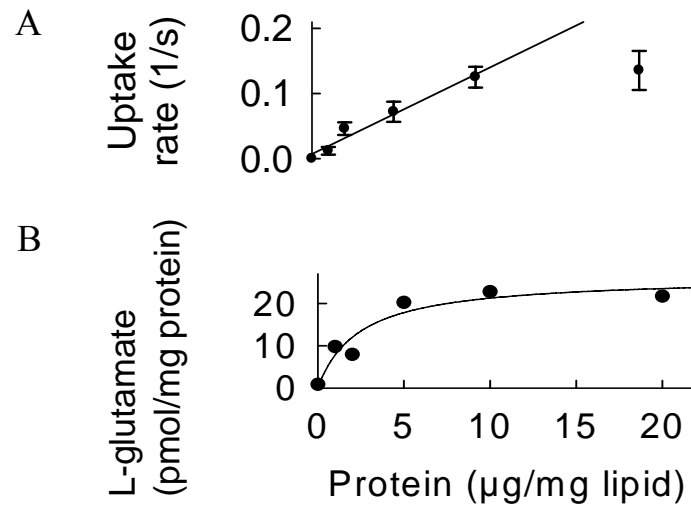


Fig. 3.5 Protein concentration-dependence of the transport rate (A) and accumulation (B) of L-[³H]-glutamate into ecglTP proteoliposomes. In (B) accumulated L-[³H]-glutamate levels were measured after 10 min of incubation (●, $n = 3$).

3.2.2 Substrate specificity of ecglTP

In order to test the specificity of the *E. coli* *glTP*-encoded glutamate transporter, the initial rates of L-[³H]-glutamate transport were determined in the presence of other potential substrates, i.e. alanine, aspartate, cysteine, cystine, and serine (Fig. 3.6.)

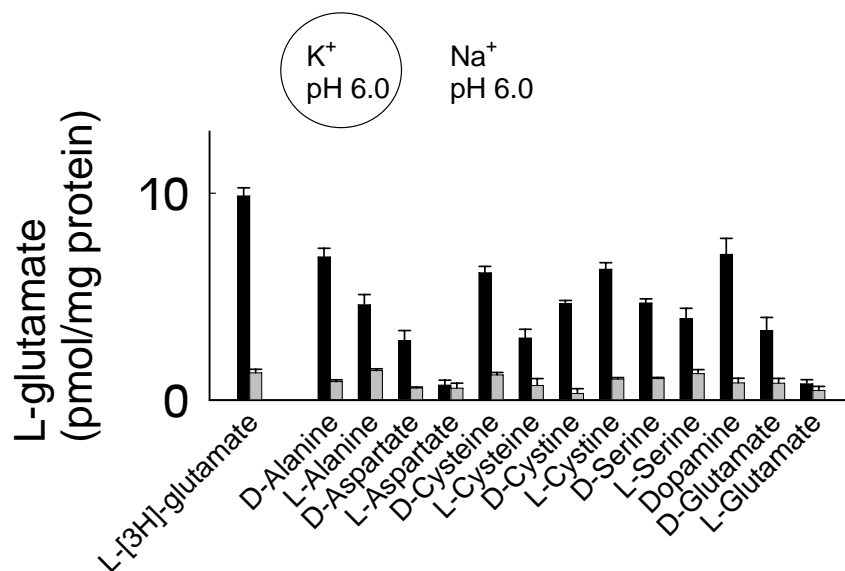


Figure 3.6 L-[³H]-glutamate uptake in the presence of various non-radioactive substrates at a concentration of 500 µM. ■ ecglTP ($n \geq 4$), ■ control ($n \geq 4$). L-[³H]-glutamate levels were measured after 10 min of incubation.

The radiotracer uptake is reduced in the presence of all potential substrates apart from D-alanine ($p < 0.01$), indicating competition between these compounds and ^3H -L-glutamate. A decrease comparable to the effect of non-radiolabeled L-glutamate was only observed for L-aspartate. A non-related neurotransmitter, dopamine, did not cause a significant reduction of radioactive glutamate fluxes, indicating a specific substrate transport by ecglTP.

In addition, the vesicular uptake of L-serine and of dopamine as a negative control was studied using radiotracer flux measurements directly (Fig. 3.7). In contrast to mammalian EAATs (Bendahian *et al.*, 2000), ecglTP does transport L- ^{14}C -serine, but in comparison to L-glutamate the serin transport is strongly reduced. Transport of radioactively labeled dopamine was not observed.

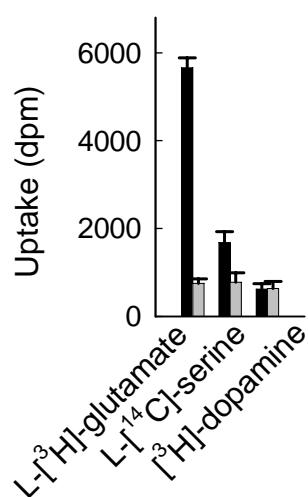


Figure 3.7 Uptake levels of $0.0175 \mu\text{M}$ L- ^3H -glutamate, L- ^{14}C -serine and ^3H -dopamine. ■ ecglTP ($n = 4$), □ control ($n = 4$). Accumulated radioactivity levels were measured after 10 min.

3.3 Cation selectivity of ecglTP

3.3.1 Glutamate uptake by ecglTP is sodium- and potassium-independent

Secondary-active transport utilizes transmembrane voltage and ion gradients. Eukaryotic glutamate transporters carry one glutamate molecule together with three Na^+ ions and one H^+ in counter-transport with one K^+ ion, resulting in the movement of two net charges per transport cycle (Levy *et al.*, 1998; Zerangue *et al.*, 1996). To assess the coupling ratio of Na^+ or K^+ to glutamate transport by ecglTP, ^3H -L-glutamate uptake in the presence of varying Na^+ or K^+ concentrations was measured. In contrast to mammalian EAATs, variation of neither the external $[\text{Na}^+]$ nor the intravesicular $[\text{K}^+]$

modifies equilibrium glutamate uptake by *ecgltP* (Fig. 3.8 A and B). A discrepancy in the uptake levels between (A) and (B) may be due to the presence of N-methyl-D-glucamine (see 2.4.2), which may have some influence on transport, as has been shown for Glt_{Ph} (Ryan *et al.*, 2009).

According to these results, it is possible to conclude that there is no change of transport activity under these conditions, indicating that the transport is not coupled to other cations beside protons.

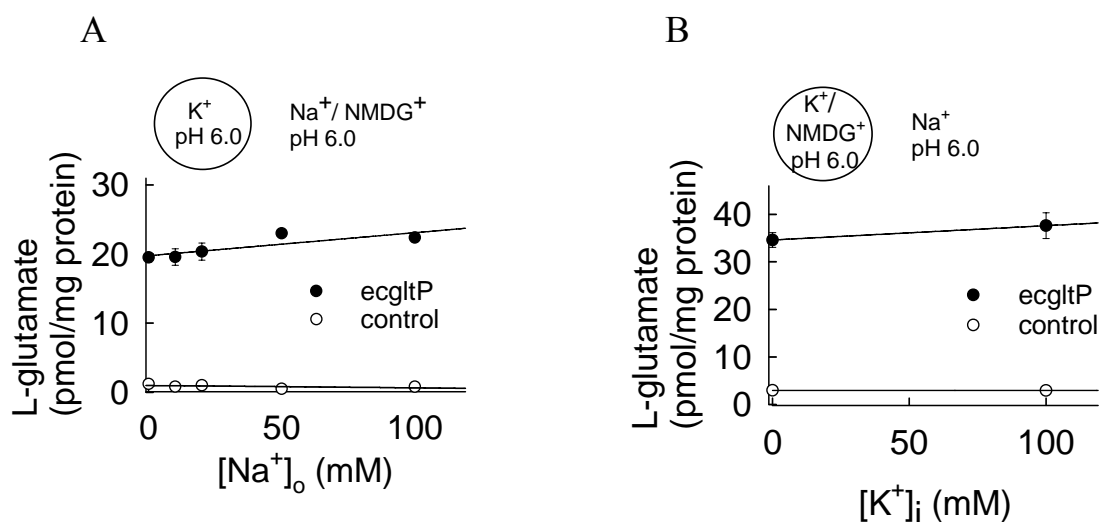


Figure 3.8 L- ^3H -glutamate uptake at various concentrations of extravesicular Na^+ (A) or intravesicular K^+ (B). Accumulated L- ^3H -glutamate levels were measured after 10 min ($n = 4$). Standard intra- and extravesicular solutions with symmetrical pH, without addition of valinomycin.

3.3.2 *ecgltP* co-transporters glutamate and H^+

Glutamate transport by the EAATs is also coupled to the co-transport of one proton (Zerangue *et al.*, 1996). To test if transport by *ecgltP* is similarly coupled to H^+ , ^3H -L-glutamate uptake in the presence of two different pH-gradients was measured (Fig. 3.9).

ecgltP-mediated glutamate uptake is dependent on the proton gradient, for two different external pHs. The application of an intravesicular pH (pH_i) of 8.0 and an external pH (pH_o) of 6.0 causes a fast glutamate accumulation that reaches equilibrium at higher internal L- ^3H -glutamate concentrations than for an external pH of 7.0. Thus, acidic pH stimulates glutamate transport and increases the steady-state concentration, indicating that *ecgltP* mediates a coupled transport of one glutamate and at least one proton.

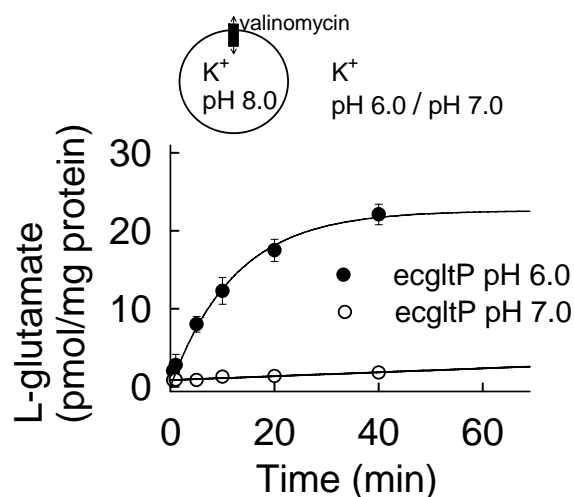


Figure 3.9 ecgltP-mediated glutamate uptake is dependent on the proton gradient, for two different external pHs. pH dependence of the time course of L-[^3H]-glutamate accumulation into ecgltP-containing proteoliposomes at pH_i 8.0 in the presence of valinomycin, ($n = 4$).

3.4 Determination of the transport stoichiometry of ecgltP

3.4.1 Electrogenicity of glutamate transport by ecgltP

Was tested, if ecgltP-mediated L-glutamate transport is an electrogenic process. For this purpose the vesicular membrane potential was modified by the addition of valinomycin and the establishment of a potassium gradient across the vesicle membrane. Valinomycin (Fig. 3.10) is a highly selective potassium ionophore. Therefore, the application of symmetrical potassium and valinomycin concentrations clamped the membrane potential of the vesicles to 0 mV, and the application of potassium internally but not externally, in presence of valinomycin hyperpolarizes the vesicle.

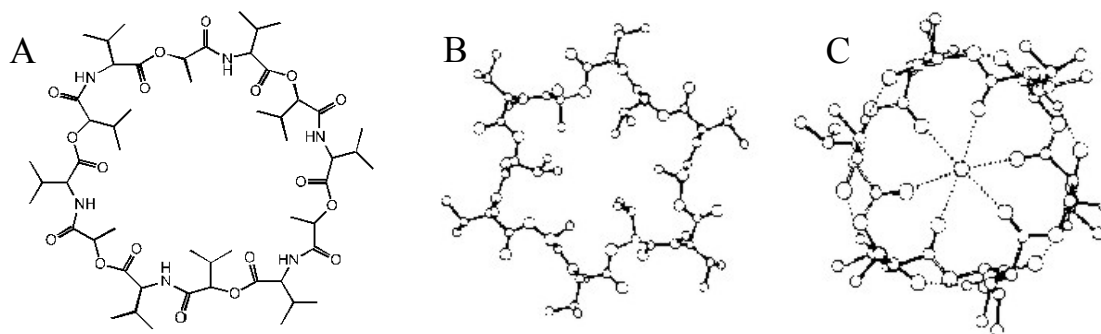


Figure 3.10 Valinomycin structure. (A) Primary structure of valinomycin. (B) Crystal structure of the free valinomycin. (C) Crystal structure of the potassium complex of valinomycin.

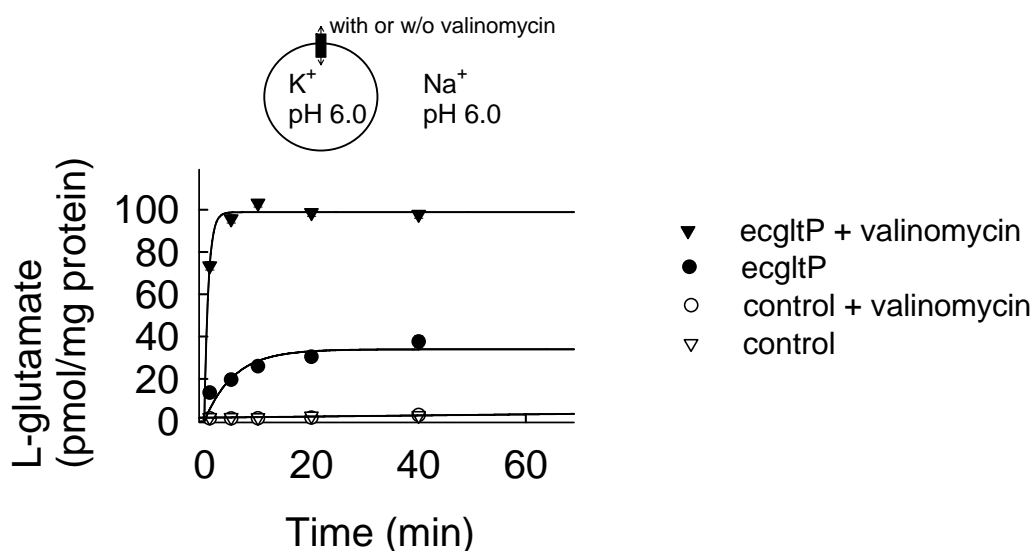


Figure 3.11 Glutamate transport by ecgltP is electrogenic. Time course of the L- $[^3\text{H}]$ -glutamate uptake at two different vesicular potentials, in the presence or absence of valinomycin, at $\text{pH}_i = 6.0$ and $\text{pH}_o = 6.0$.

With a K^+ -free external solution, permeabilization of the liposomes with valinomycin causes a passive efflux of K^+ and hyperpolarizes the vesicle interior. At a symmetrical pH of 6.0, such a process results in increases in both the speed of uptake and steady state level of the radioactive glutamate (Fig. 3.11). The conclusion is that glutamate uptake is associated with the movement of positive charges across the membrane. Since glutamate is negatively charged, glutamate transport must be coupled to the movement of at least two protons.

3.4.2 Determination of the coupling stoichiometry of ecgltP by the static head method

H^+ /glutamate symport terminates when the electrochemical gradients for protons and glutamate compensate for each other. The relationship between the equilibrium concentrations is given by equation (1):

$$\frac{[\text{glutamate}]_i}{[\text{glutamate}]_o} = \left(\frac{[\text{H}^+]_o}{[\text{H}^+]_i} \right)^n e^{-(n-1)e\phi / kT} \quad (1)$$

Where V represents the transmembrane voltage and n the transport stoichiometry or coupling coefficient, i.e. the number of H^+ coupled to the transport of one glutamate.

In a semilogarithmic plot, this equation predicts a linear relationship between the accumulated radioactivity and the calculated transmembrane potential, with a slope of $n-1$.

Next, to determine the coupling coefficient the static head method was employed (Fukuhara *et al.*, 1984; Turner, 1985), see also 2.4.2. Vesicles were first loaded with L- $[^3\text{H}]$ -glutamate and kept in an external medium with the same concentration of labeled glutamate as in the loaded vesicles. After establishing an outwardly directed 1:10 glutamate gradient by 1:9 dilution into solutions with variable pHs, the change of intravesicular L- $[^3\text{H}]$ -glutamate concentration over time was measured (Fig. 3.12 A). In these experiments, vesicles were clamped to 0 mV using symmetrical K^+ and valinomycin.

The net substrate flux depends on the glutamate and the proton gradients and will be zero at ionic conditions at which the driving force for the coupled transport is zero:

$$\frac{[\text{glutamate}]_i}{[\text{glutamate}]_o} = \left(\frac{[\text{H}^+]_o}{[\text{H}^+]_i} \right)^n \quad (2)$$

or

$$\log \frac{[\text{glutamate}]_i}{[\text{glutamate}]_o} = n(\text{pH}_i - \text{pH}_o) \quad (3)$$

Under the conditions applied here, this can be simplified to:

$$n(\text{pH}_i - \text{pH}_o) = 1 \quad (4)$$

At an extravesicular pH of 6.0, glutamate is transported into the vesicles, whereas glutamate moves out of the vesicle at a pH_o of 6.8 (Fig. 3.12 A). Glutamate transport by ecglTP is very slow under these conditions, preventing an accurate determination of the time constants and steady-state values of intravesicular glutamate concentrations. However, vesicular glutamate concentrations obtained in this experiment allow determination of the pH at which the H^+ /glutamate transport is at

equilibrium. Figure 3.12 (B) gives the normalized glutamate accumulation on a logarithmic scale for three different pH_o values 20 minutes after dilution of the vesicles.

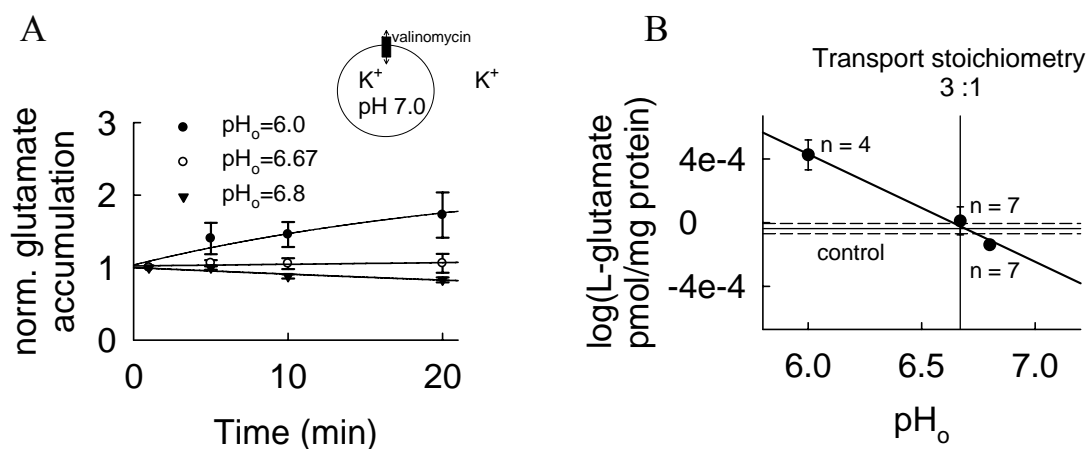


Figure 3.12 Static head experiment. (A) Time course of the normalized intravesicular L-[³H]-glutamate concentration at three external pHs after 1:9 dilution in a static head experiment. (B) Plot of the vesicular L-[³H]-glutamate, measured 20 min after dilution, from the experiments shown in (A), versus the external pHs. The solid line gives mean values from control vesicles, the dashed lines control mean values \pm SEM.

The pH dependence is well described by a straight line that crosses the x-axis at pH 6.67. Measurements 10 min after dilution produced similar results (data not shown), indicating that H⁺/glutamate symport is at equilibrium at pH 6.67. The conclusion is that, under the tested experimental conditions, ecglTP sustains a coupled transport of three protons and one glutamate.

3.4.3 Determination of the coupling stoichiometry of ecglTP by voltage dependence measurements

In order to determine the coupling stoichiometry of the H⁺/glutamate symport, the glutamate uptake was compared at different membrane potentials. Vesicular potentials were modified by variation of the extravesicular K⁺ concentration in the presence of 2.5 μM valinomycin, to produce potentials of -20 mV, -37 mV, and -50 mV. Reduction of $[\text{K}^+]_o$ resulted in increased uptake rates and steady state glutamate accumulations after 40 min of incubation. The voltage dependence of glutamate transport (Fig. 3.13) allowed the determination of the number of protons that are co-transported with one glutamate by ecglTP.

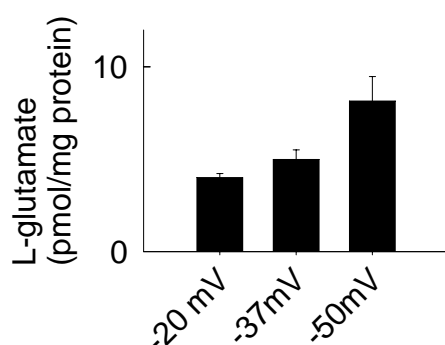


Figure 3.13 Voltage dependence of glutamate transport by ecglP. Vertical bars show the accumulated glutamate at steady state, after 40 min of incubation at different voltages ($n = 4$), ecglP.

For a coupled transporter that only transports protons and glutamate, as is the case for ecglP, the ratio of intravesicular glutamate to extravesicular glutamate depends on the transmembrane proton gradient and voltage (equation 1, see 3.4.2). This relationship can be expressed using a logarithmic plot of the intravesicular glutamate concentration versus the transmembrane voltage. The linear fit (Fig. 3.14) to this relationship (equation 1) gives the number of co-transported protons. The red lines show the predicted glutamate accumulation, assuming a coupling ratio of 3 or 2 co-transported protons. The voltage dependence of the accumulated glutamate concentration reveals that three protons are co-transported with one glutamate by ecglP.

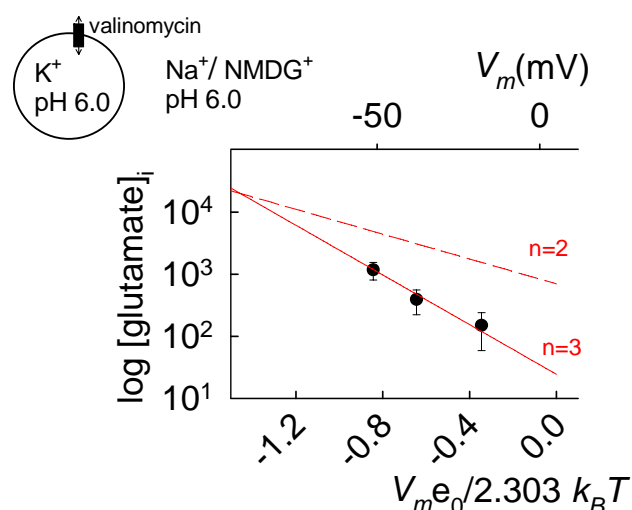


Figure 3.14 Coupling stoichiometry of ecglP. Predicted glutamate accumulation assuming a coupling ratio of 3 or 2 co-transported protons (red lines), (●) plotted from Fig. 3.13 data of the voltage dependence of glutamate transport by ecglP.

3.5 Temperature dependence of eglT_P-mediated glutamate uptake

Active transport mechanisms are processes, which are required for the uphill movement of substrates. Temperature coefficients (Q_{10}) and apparent activation energies (E_A) are obtainable by extraction from individual transport rates using the Arrhenius equation (see also 2.5.4). For this purpose, the rate of glutamate accumulation at various temperatures (Fig. 3.15) was measured. Under described conditions experiments indicate that the uptake rates increase with temperature with a Q_{10} of 8. An Arrhenius plot of transport rates with hyperpolarized vesicular potentials (Fig. 3.16), demonstrates that glutamate transport is associated with an apparent activation energy of 160 kJ/mol.

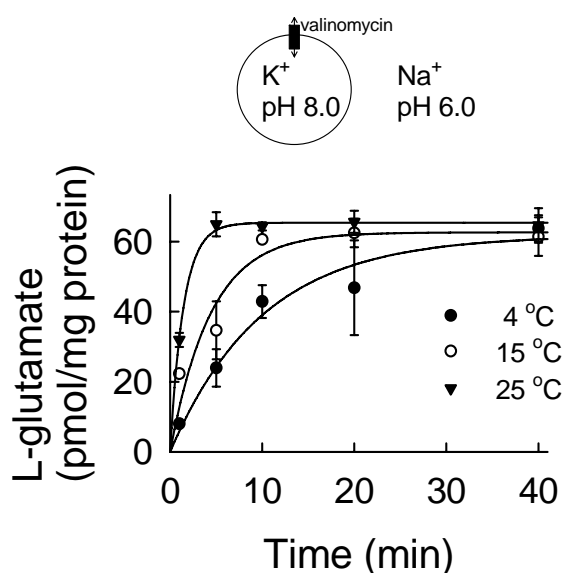


Figure 3.15 Temperature dependence of eglT_P glutamate transport. Time course of L-[³H]-glutamate accumulation in vesicles at three different temperatures ● 4 °C ($n = 4$), ○ 15 °C ($n = 4$), and ▼ 25 °C ($n = 4$).

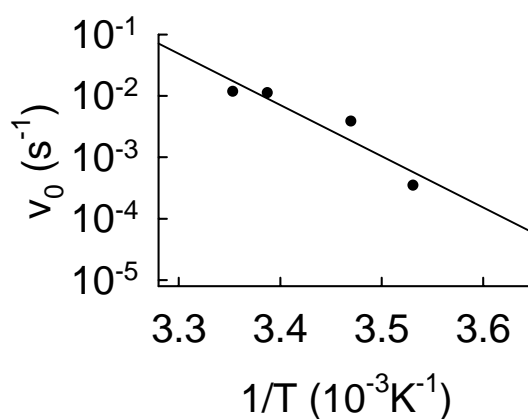


Figure 3.16 Arrhenius plot for initial transport rates. Plot based on data shown in Fig. 3.15.

3.6 Characterization of N401D ecgltP

3.6.1 N401D ecgltP mediates glutamate/aspartate transport into liposomes

N401D ecgltP contains an aspartate residue at a position homologous to D405 of Glt_{ph}, which was shown to be crucial for sodium binding (Boudker *et al.*, 2007). The time course of radioactive glutamate accumulation by proteoliposomes containing purified N401D ecgltP in standard intravesicular and extravesicular solutions (see 2.4.2) is shown in Fig. 3.17 A. Control experiment was carried out in parallel using vesicles without the ecgltP protein. Because N401D ecgltP dramatically reduces the transport rate of L-glutamate (Fig. 3.17), for the following experiments L-aspartate with a higher transport rate was used as a substrate. Furthermore, in order to get uptake rates of N401D ecgltP significantly above the control level, it was also necessary to modify the membrane potential and to increase a protein/lipid ratio to 45 $\mu\text{g}/\text{mg}$ (2.4.1). Figure 3.17 B shows values of the accumulated radioactivity after 40 min of incubation for WT ecgltP and N401D ecgltP with two different substrates (glutamate or aspartate).

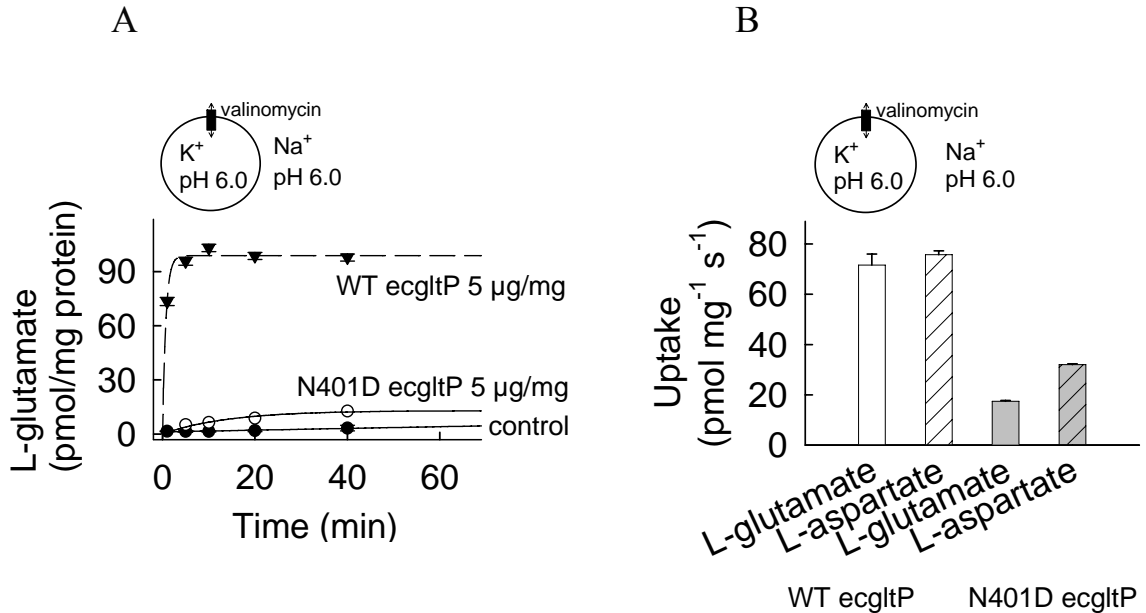


Figure 3.17 Substrate transport into proteoliposomes via N401D ecgltP. (A) Time courses of the L-^{[3]H}-glutamate uptake at negative vesicular potentials, in the presence of valinomycin, at symmetrical pH = 6.0. (\blacktriangledown) WT ecgltP ($n = 3$), (\circ) N401D ecgltP ($n = 2$), and (\bullet) control were vesicles without protein ($n = 4$). A protein/lipid ratio of 15 $\mu\text{g}/\text{mg}$ for WT ecgltP and N401D ecgltP was used. (B) Graphs show values of the accumulated radioactivity after 40 min of incubation with two different substrates, WT ecgltP ($n = 4$) and N401D ecgltP ($n = 4$). Control uptake values were subtracted. Protein/lipid ratios of 15 $\mu\text{g}/\text{mg}$ for WT ecgltP and 45 $\mu\text{g}/\text{mg}$ for N401D ecgltP were used.

3.6.2 N401D ecgltP mediates electrogenic co-transport of substrate and protons

To test if transport by N401D ecgltP is similarly coupled to H^+ as by WT ecgltP, 3H -L-aspartate uptake in the presence of various pH-gradients was performed (Fig. 3.18). N401D ecgltP-mediated glutamate uptake is dependent on the proton gradient. The application of an intravesicular pH of 6.0 and an external pH of 6.0 causes a fast glutamate accumulation that reaches equilibrium at higher internal L- 3H -aspartate concentrations than for other external pHs. Again, acidic pH stimulates substrate transport and increases the steady-state concentration, indicating that N401D ecgltP mediates a coupled transport of one glutamate and at least one proton.

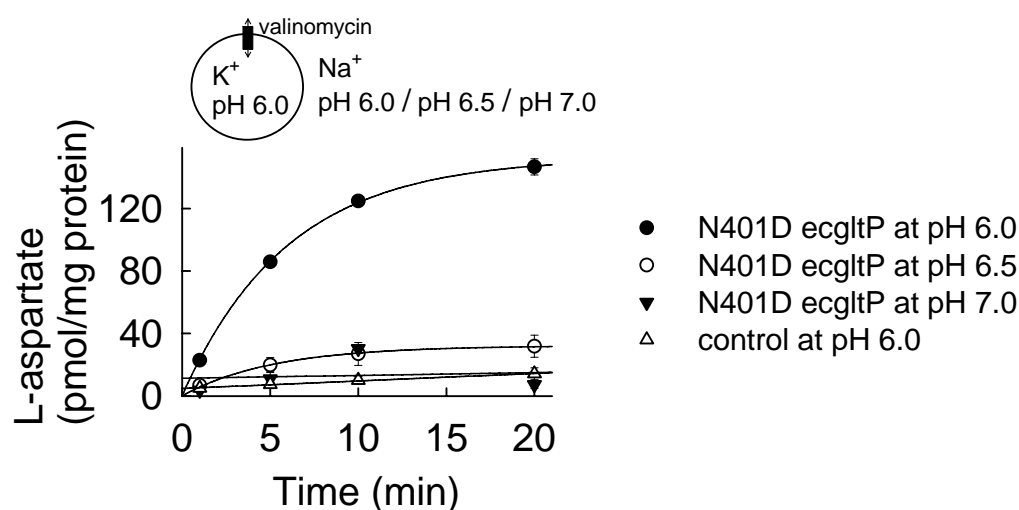


Figure 3.18 N401D ecgltP co-transporters aspartate and H^+ . pH dependence of the time course of L- 3H -aspartate accumulation in N401D ecgltP-containing proteoliposomes at pH_i 8.0, in the presence of valinomycin, vesicles without protein were used as a control ($n = 3$).

Glutamate transport by WT ecgltP is electrogenic. In order to determine, if N401D ecgltP-mediated substrate transport is also an electrogenic process following experiments were performed. Figure 3.20 shows time courses of the accumulated glutamate at different voltages. Vesicles without protein were used as a control. Data demonstrate, that substrate transport via N401D ecgltP is also an electrogenic process. Since aspartate carries a net single negative charge, the aspartate co-transport via N401D ecgltP must be coupled to the movement of at least two positive charges.

3.6.3 Aspartate uptake by N401D ecglpP is Na⁺-independent

This mutant was designed with the expectation of finding a sodium dependent transport mechanism, lacking in the WT ecglpP. However, aspartate uptake by N401D ecglpP is sodium independent (Fig. 3.19). This indicates that the negative charge that is found in the homologous position in Gltp_h is not alone responsible for Na⁺-coupling.

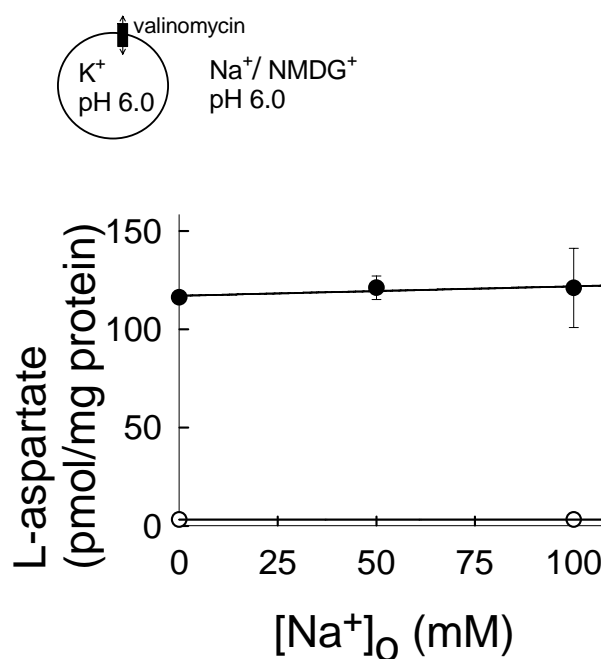


Figure 3.19 L-[³H]-aspartate uptake via N401D ecglpP at various concentrations of extravesicular Na⁺. Standard intra- and extravesicular solutions with symmetrical pH and 2.5 μM valinomycin were applied. Accumulated L-[³H]-aspartate levels were measured after 40 min ($n = 4$).

3.6.4 Determination of the coupling stoichiometry of N401D ecglpP by voltage dependence measurements

As was shown for the wild type ecglpP (Fig. 3.13 and 3.14), voltage dependence of glutamate transport allowed the determination of the number of protons that are co-transported with one glutamate by N401D ecglpP. In order to determine the coupling stoichiometry of the H⁺/glutamate symport via N401D ecglpP the same method of voltage dependence measurements (see also 3.4.3) was applied (Fig. 3.20, Fig. 3.21).

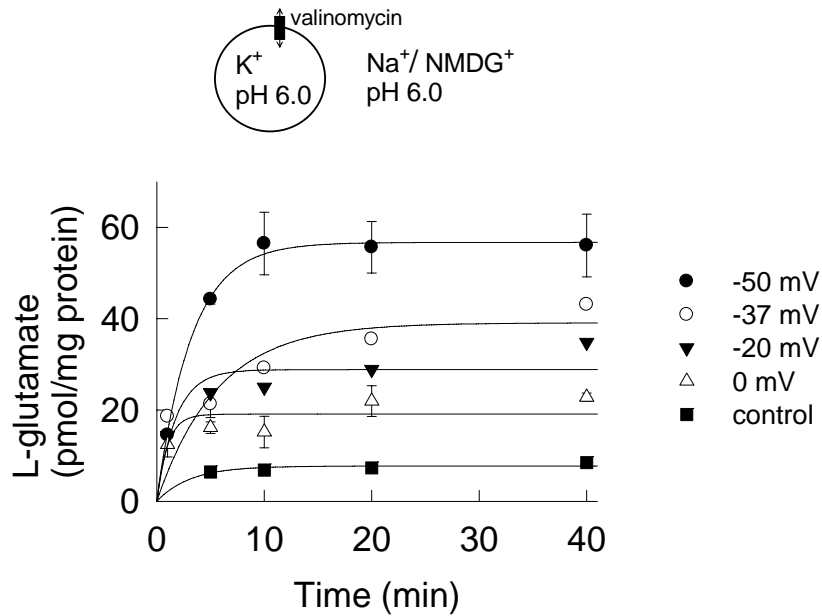


Figure 3.20 The voltage dependence of glutamate transport by N401D ecgltP. Time courses of the accumulated glutamate at different voltages are demonstrated ($n = 4$).

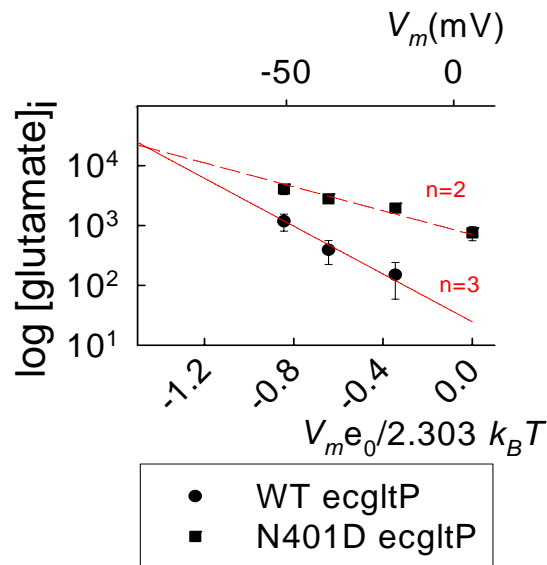


Figure 3.21 Coupling stoichiometry of WT ecgltP and N401D ecgltP. Predicted glutamate accumulation assuming a coupling ratio of 3 or 2 co-transported protons (red lines). Plotted data of the voltage dependence at steady state (after 40 min of incubation) of glutamate transport by WT ecgltP (from Fig. 3.13) and by N401D ecgltP (from Fig. 3.20).

The voltage dependence of the glutamate accumulation by N401D ecglP reveals that, in contrast to the wild type, the mutant transports one glutamate stoichiometrically coupled to two protons. Obviously, N401 residue plays a role in defining the number of co-transported protons in ecglP.

4. Discussion

Glutamate transport proteins play a crucial role in both eukaryotic and prokaryotic cells. Although their functions in both kingdoms are very different, the correlation of the conclusions from mutagenesis experiments on eukaryotic glutamate transporters with the high-resolution structure of a prokaryotic glutamate transporter Glt_{Ph} from *Pyrococcus horikoshii* indicates that eukaryotic and prokaryotic glutamate transporters share a common architecture, sequence, oligomerisation state, structure, and basic mechanism of transport. However, little is known about the functional mechanisms of the prokaryotic transporters. The *gltP* gene of *Escherichia coli* encodes a protein homologous to the mammalian EAAT-type glutamate transporters. The study of *ecgltP* allows the application of molecular, functional, and biochemical methods to elucidate the molecular mechanisms underlying coupled transport by this glutamate transporter. The transport mechanisms determined for *ecgltP* may be similar to those in its eukaryotic homologues, and thus it may be possible to extrapolate from the information obtained in this study to gain a better understanding of the molecular determinants of coupled transport by eukaryotic glutamate transporters. In this thesis, a detailed functional characterization of *ecgltP* is presented, where the ion dependence of this glutamate transporter is described. Like the EAATs, glutamate transport by *ecgltP* is coupled to the co-transport of H⁺. In contrast to the EAATs, this process is not coupled to the co-transport of Na⁺ ions or the counter-transport of K⁺ ions.

4.1 Purified and reconstituted *ecgltP* mediates glutamate uptake into proteoliposomes

After expression in *E. coli*, *ecgltP* was purified by one affinity chromatography step from bacteria and then eluted predominantly as a single symmetrical peak (Fig. 3.3 B), indicating that the majority of the purified protein (>95 %) exists in one oligomeric conformation. The use of 1 mM DDM detergent in the protein purification procedure conserves the native trimeric subunit stoichiometry of *ecgltP* (Gendreau *et al.*, 2004). Purified *ecgltP* was reconstituted in artificial lipid vesicles. Radiotracer flux measurements into *ecgltP*-containing proteoliposomes were then used to characterize the transport properties of *ecgltP*. Reconstitution experiments demonstrated that *ecgltP* was able to sustain coupled transport. The dependence of L-[³H]-glutamate accumulation – determined after 10 min – on the protein/lipid ratio is well described by a mono-exponential function (Fig. 3.5 B), as expected for a Poisson distribution

(Heginbotham *et al.*, 1998). It was shown that glutamate transport by ecgltP is electrogenic (Fig. 3.11 A, Fig. 3.11 B) and depends only on the proton concentrations on both sides of the membrane (Fig. 3.9), but is not affected by the presence, absence or concentration of Na⁺ (Fig. 3.8 A) or K⁺ (Fig. 3.8 B). ecgltP has already been studied using radiotracer flux experiments with cytoplasmic bacterial membrane vesicles or whole bacteria cells after the overexpression in *E. coli* (Deguchi *et al.*, 1989; Wallace *et al.*, 1990). In both reports, as well as in this work, a sodium-independent, electrogenic uptake of glutamate was reported. The conditions of protein purification and reconstitution and the method of performing the functional tests therefore do not modify the transport properties of ecgltP. The techniques used in the work presented here allowed the study of ecgltP in artificial liposomes without possible contamination by other cellular components.

4.2 ecgltP has less substrate specificity than eukaryotic EAAT glutamate transporters

ecgltP is mainly selective for glutamate and aspartate (Fig. 3.6, Fig. 3.7) but also sustains a secondary-active transport for alanine, cysteine, cystine, and serine, albeit with a lower affectivity. This property contrasts with the specificity of the EAAT glutamate transporters (Danbolt, 2001).

This difference between prokaryote and eukaryote substrate specificity makes sense in light of the fact that glutamate transporter function in both kingdoms is different. Little is known about the biological function of ecgltP but one may speculate that the reason for such a broad spectrum of transported substrates, is that as bacterial glutamate transporter proteins are nutrition transporters, it is beneficial for the bacteria not only to accumulate glutamate (Halpern *et al.*, 1965) but also other amino acids.

4.3 Stoichiometry of ecgltP: three protons are electrogenically co-transported with one glutamate

In marked contrast to mammalian glutamate transporters and to some other bacterial glutamate transporters, transport by ecgltP does not depend on sodium (Fig. 3.8 A) or potassium (Fig. 3.8 B). Glutamate transport by purified ecgltP is therefore not energetically coupled to the movement of these ions, in agreement with earlier results

on cytoplasmic bacterial membranes and on whole bacteria (Deguchi *et al.*, 1989; Wallace *et al.*, 1990) or on purified and reconstitution in *E. coli* lipids glutamate transporter GltT from *Bacillus stearothermophilus* (Gaillard *et al.*, 1996). GltT-mediated glutamate transport has also been reported as independent of external $[\text{Na}^+]$.

The results presented here demonstrate that ecgltP-mediated H^+ :glutamate co-transport is electrogenic (Fig. 3.11), with a coupling stoichiometry of 3:1 (Fig. 3.12, Fig. 3.14). Two different methods were applied to determine the coupling stoichiometry of ecgltP: the static head method (Fukuhara *et al.*, 1984; Turner, 1985) and measurements of the voltage dependency of accumulated substrate at the steady state. Both techniques produced the same result and showed that three protons are co-transported together with one glutamate by ecgltP, demonstrating that the properties of Na^+ co-transport and K^+ counter-transport with glutamate are not conserved between evolutionarily distant members of the glutamate transporter family: ecgltP and EAATs.

This is especially interesting because ecgltP lacks a glutamate residue at position 320. In GLT-1, the rat homolog of EAAT2, a glutamate residue at the equivalent position (E404) was proposed to bind K^+ (Kavanaugh *et al.*, 1997). The demonstrated K^+ -independence of glutamate transport via ecgltP and the absence of this residue in ecgltP are consistent with that proposed role of this glutamate residue as a K^+ acceptor. On the other hand, in another isoform – EAAT3 – the same residue was proposed to be responsible for H^+ binding (Greuer *et al.*, 2003). ecgltP transports three protons without having a glutamate residue at this position, demonstrating that this binding site is not conserved between mammalian and prokaryotic glutamate transporters.

4.4 Determination of unitary transport rates and temperature dependence of ecgltP-mediated glutamate uptake

Secondary-active transporters are usually thought to function using an alternating access mechanism (Jardetzky, 1966; Kavanaugh, 1998). In this canonical transport scheme, one or more permeation pathways possess gates at the intra- and extracellular sides of the plasma membrane. These gates are never simultaneously open, but instead open sequentially to allow alternating access to the cytoplasmic and extracellular compartments. An alternative mechanism for secondary-active transport is one in which multiply-occupied channels contain a variety of substrates moving in single-file (Läuger, 1979; Läuger, 1980; Su *et al.*, 1996; DeFelice *et al.*, 2001). In such

transport processes, ions move when another ion enters the pore from either direction, and this coupling of substrate transport is capable of sustaining the channel-mediated transport of one substrate against its electrochemical gradient. Alternating access and channel-like transporters differ in their transport rates and in the conformational changes necessary for substrate transport. In this study, the unitary transport rates and the temperature dependence of ecglP-mediated glutamate transport were therefore determined to define the mechanism used by the ecglP transporter (see 2.4.3 and 3.5).

The ecglP transporter consists of three subunits (Gendreau *et al.*, 2004), each of which has been shown to be able to transport glutamate independently (Yernool *et al.*, 2004; Grewer *et al.*, 2005; Koch *et al.*, 2005). Time course measurements of radioactive glutamate accumulation and the calculation of the number of ecglP subunits present in the tested vesicle sample, yielded an estimate of a transport rate of 4 glutamate molecules/sec at 0 mV vesicle potential and of 62 molecules/sec for a hyperpolarized membrane potential achieved by adding valinomycin to a K⁺-free external solution. This is closely similar to the values for mammalian EAAT glutamate transporters of 1.3 molecules s⁻¹ for purified rat glutamate transporters (Danbolt *et al.*, 1990) and between 4 and 27 molecules s⁻¹ for human EAAT2 heterologously expressed in *Xenopus* oocytes (Wadiche *et al.*, 1995).

Measurements of ecglP uptake were performed at different temperatures (4 °C, 15 °C and 25 °C) (Fig. 3.15). Based on this data an Arrhenius plot (see 2.4.3., 3.5 and Fig. 3.16) of transport rates with hyperpolarized vesicular potentials demonstrates that glutamate transport is associated with an apparent activation energy of 160 kJ/mol. The apparent activation energy of glutamate transport is much larger than values characteristic for diffusion-limited processes (Hille, 1992) and strongly supports a transport mechanism that involves large conformational changes of the transport protein. Measurements of individual transport rates and their temperature dependence indicated a transport process that encompasses major conformational changes, consistent with alternating access models. Glutamate transport by ecglP can therefore be considered to be associated with major conformational changes of the protein and resembles transport by mammalian homologues in general.

The temperature dependence data and measurements of individual transport rates support the notion that conformational changes are associated with the ecglP transport mechanism, which is also in agreement with the results of functional characterization of Glt_{Ph} (Ryan *et al.*, 2009).

4.5 Characterization of N401D ecgltP

The aspartate at position 405 of Glt_{ph} and the homologous residues in other glutamate transporters are known to bind Na⁺ during the glutamate transport process (Tao *et al.*, 2006, Tao *et al.*, 2007; Boudker *et al.*, 2007). In wild type ecgltP, this residue is exchanged to asparagine. To elucidate the role of this residue in ecgltP, a mutant – N401D ecgltP – bearing the conserved aspartate at this position was studied.

Transport by N401D ecgltP does not depend on sodium (Fig. 3.19). This finding demonstrates that coupling of glutamate and Na⁺ transport cannot be transplanted from mammalian EAATs, or from Glt_{ph} to ecgltP by inserting a single negative charge and also that other amino acids take part in Na⁺ transport and that the molecular requirements for coupled sodium-glutamate transport are more complex than currently thought.

The voltage dependency of the glutamate accumulation by the N401D ecgltP mutant reveals that, in contrast to the wild type ecgltP, which mediates the stoichiometrically coupled co-transport of one glutamate and three protons, N401D ecgltP presents voltage-dependent transport of one glutamate stoichiometrically coupled to two protons (Fig. 3.20, Fig. 3.21).

Surprisingly, instead of changing the glutamate transport to a Na⁺-dependent mechanism the introduction of aspartate at this position (N401) altered the H⁺:glutamate transport stoichiometry to 2:1. Moreover, N401 plays an additional role in defining the number of co-transported protons in ecgltP. It appears possible that D401 acts as a possible binding site for protons. One could imagine that the incorporated aspartate increases affinity for one proton. The proton can no longer dissociate, but remains bound and is therefore not transported.

4.6 Conclusions

The functional characterization of ecglT transporter presented in this study demonstrates that:

- Na^+ co-transport and K^+ counter-transport are not conserved between ecglT and EAATs.
- ecglT mediated H^+ :glutamate co-transport has a coupling stoichiometry of 3:1.
- substantial conformational changes are associated with ecglT transport function, supporting an alternating access model.
- residue N401 plays a role in defining the number of co-transported protons in ecglT.
- coupling of glutamate and Na^+ transport can not be transplanted to ecglT by inserting a single negative charge at position 401.
- ecglT represents a model to study the mechanisms underlying glutamate transport and coupled transport in general. The existence of such a protein model provides a good system to test hypotheses concerning different steps in the glutamate uptake cycle.

4.7 Further research

Glutamate transporter proteins are still incompletely understood. The bacterial glutamate transporter from *E. coli* – ecgltP – represents an interesting model to study glutamate transport. A complete understanding of Na⁺- and K⁺-binding sites in mammalian isoforms could potentially be achieved by transferring these sites to ecgltP mutants. Performing such experiments using ecgltP would thus help future understanding of coupled transport in EAATs.

In addition, interesting questions are still open regarding the oligomerisation state of the protein and its influence on the mechanism of glutamate uptake. The ecgltP transporter consists of three subunits (Gendreau *et al.*, 2004) each of which are able to transport glutamate independently (Yernool *et al.*, 2004; Grewer *et al.*, 2005; Koch *et al.*, 2005). The detergent DDM conserves the native trimeric subunit stoichiometry (Gendreau *et al.*, 2004), while LDAO disrupts this assembly and produces a monodispersed fraction of monomeric ecgltP. Producing by applying of different detergents in purification procedure or by mutagenesis and comparing functional properties of the two types of ecgltP transporters – trimers and monomers – could give information about the impact of oligomerisation on transport functions.

5. Abstract

5.1 Abstract, English

Functional characterization of a glutamate transporter from *Escherichia coli*

Glutamate is the major excitatory neurotransmitter in the mammalian CNS. After its release from glutamatergic nerve terminals, glutamate is rapidly taken up into glial and neuronal cells by mammalian Na⁺-dependent glutamate transporters (excitatory amino acid transporters 1 to 5, EAATs). In recent years, various EAAT paralogs have been identified in prokaryotes and shown to exhibit different transport stoichiometries. Whereas EAATs transport 3 Na⁺, 1 H⁺, and 1 glutamate in countertransport with 1 K⁺, there are bacterial paralogs that only transport glutamate/aspartate stoichiometrically coupled to H⁺, or to Na⁺. The simplicity of the transport stoichiometry of bacterial transporters might allow transplantation of transport mechanisms from one isoform to the other and thus provide insights into molecular determinants of coupled transport. Radiotracer flux accumulation by purified and reconstituted glutamate transporter from *E. coli* (ecgltP) was studied. In marked contrast to mammalian EAATs, glutamate transport by ecgltP is independent of Na⁺ and K⁺. ecgltP transports H⁺ and glutamate, and the voltage dependence of radiotracer flux accumulation allowed the determination of a transport stoichiometry of one glutamate coupled to three protons. Measurements of individual transport rates of ecgltP and their temperature dependence demonstrated a transport process that encompasses major conformational changes, consistent with alternating access models. WT ecgltP was characterized in comparison to the N401D ecgltP mutation. In sodium-dependent aspartate transporters, a conserved aspartate in TM8 (D405 in Glt_{ph}) is known to bind Na⁺ during the glutamate transport process. In ecgltP an asparagine is present instead of aspartate. Insertion of this candidate binding site into ecgltP does not convert this into a sodium-coupled glutamate transporter. It solely reduces the number of cotransported protons from 3 to 2. This finding demonstrates that coupling of glutamate and Na⁺ transport cannot be transplanted from mammalian EAATs to ecgltP by inserting a single negative charge and also that other amino acids take part in Na⁺ transport and that the molecular requirements for coupled sodium-glutamate transport are more complex than currently thought.

Keywords:

glutamate transporters, ecgltP, EAATs

5.2 Zusammenfassung

Funktionelle Charakterisierung eines Glutamattransporters aus *Escherichia coli*

Die Aminosäure L-Glutamat ist der wichtigste exzitatorische Neurotransmitter im zentralen Nervensystem von Säugetieren. Glutamat wird nach der Freisetzung aus glutamatergen Nervenendigungen durch Natrium abhängige exzitatorische Aminosäuretransporter (excitatory amino acid transporters 1-5, EAAT) in gliale und neuronale Zellen aufgenommen. In den vergangenen Jahren wurden in Prokaryoten verschiedene EAAT Paraloge identifiziert, die sich in der Transportstöchiometrie von Säugetierisoformen unterscheiden. Während eukaryotische Transporter (EAATs) drei Natriumionen, ein Proton und ein Glutamat im Gegentransport mit einem Kaliumion transportieren, ist in prokaryotischen Transportern der Transport eines Glutamats / Aspartats nur an Protonen oder nur an Natriumionen gekoppelt.

In dieser Studie wurde ein Glutamattransporter aus *E. coli* (ecglTP) mit Hilfe von Radiotracerflux-Techniken untersucht. EcglTP transportiert Glutamat zusammen mit Protonen. Aus der Spannungsabhängigkeit der Glutamatakkumulation konnte ein Kopplungskoeffizient von einem Glutamat zu drei Protonen bestimmt werden. Um die molekularen Determinanten des gekoppelten Transports besser zu verstehen, wurde eine potenzielle Natriumbindungsseite aus eukaryotischen Transportern in ecglTP imitiert. EcglTP unterscheidet sich u.a. in dieser potenziellen Natriumbindungsstelle von natriumabhängigen Glutamattransportern. Die Modifikation dieses potenziellen Bindungsplatzes durch eine Punktmutation (N401D) ist jedoch nicht ausreichend für einen natriumgekoppelten Glutamattransport in ecglTP. N401D ecglTP weist weiterhin eine Natrium-unabhängige Stöchiometrie mit einem Glutamat und zwei Protonen auf. Dies zeigt, dass ecglTP, auch wenn alle bekannten Natriumbindungsplätze durch molekulare Modifikationen vorhanden sind, immer noch keine Natriumionen transportieren kann, und dass die molekularen Anforderungen für den gekoppelten Natrium-Glutamat-Transport komplexer sind, als bisher angenommen.

Stichwörter:

Glutamattransporter, ecglTP, EAATs

6. References

Amara, S. G., Fontana, A. C. (2002) Excitatory amino acid transporters: keeping up with glutamate. *Neurochem. Int.* **41**: 313-318.

Arriza, J. L., Eliasof, S., Kavanaugh, M. P., Amara, S. G. (1997) Excitatory amino acid transporter 5, a retinal glutamate transporter coupled to a chloride conductance. *Proc. Natl. Acad. Sci. USA* **94**: 4155-4160.

Arriza, J. L., Fairman, W. A., Wadiche, J. I., Murdoch, G. H., Kavanaugh, M. P., Amara, S. G. (1994) Functional comparisons of three glutamate transporter subtypes cloned from human motor cortex. *J. Neurosci.* **14**: 5559-5569.

Arriza, J. L., Kavanaugh, M. P., Fairman, W. A., Wu, Y. N., Murdoch, G. H., North, R. A., Amara, S. G. (1993) Cloning and expression of a human neutral amino acid transporter with structural similarity to the glutamate transporter gene family. *J. Biol. Chem.* **268**: 15329-15332.

Barbour, B., Brew, H., Attwell, D. (1991) Electrogenic uptake of glutamate and aspartate into glial cells isolated from the salamander (*Ambystoma*) retina. *J. Physiol.* **436**: 169-93.

Bendahan, A., Armon, A., Madani, N., Kavanaugh, M. P., Kanner, B. I. (2000) Arginine 447 plays a pivotal role in substrate interactions in a neuronal glutamate transporter. *J. Biol. Chem.* **275**: 37436-37442.

Berger, U. V., Hediger, M. A. (1998) Comparative analysis of glutamate transporter expression in rat brain using differential double in situ hybridization. *Anat. Embryol. (Berl)* **198**: 13-30.

Bergles, D. E., Diamond, J. S., Jahr, C. E. (1999) Clearance of glutamate inside the synapse and beyond. *Curr. Opin. Neurobiol.* **9**: 293-298.

- Billups, B., Rossi, D., Attwell, D. (1996) Anion conductance behavior of the glutamate uptake carrier in salamander retinal glial cells. *J. Neurosci.* **16**: 6722-6731.
- Boudker, O., Ryan, R. M., Yernool, D., Shimamoto, K. and Gouaux, E. (2007) Coupling substrate and ion binding to extracellular gate of a sodium-dependent aspartate transporter. *Nature* **445**: 387-393.
- Broer, S., Brookes, N. (2001) Transfer of glutamine between astrocytes and neurons. *J. Neurochem.* **77**: 705-719.
- Chenna, R., Sugawara, H., Koike, T., Lopez, R., Gibson, T.J., Higgins, D.G., Thompson, J.D. (2003) Multiple sequence alignment with the Clustal series of programs. *Nucleic Acids Res.* **31**: 3497-500.
- Choi, D. W., Maulucci-Gedde, M., Kriegstein, A. R. (1987) Glutamate neurotoxicity in cortical cell culture. *J. Neurosci.* **7**: 357-368.
- Clements, J. D. (1996) Transmitter timecourse in the synaptic cleft: its role in central synaptic function. *Trends Neurosci.* **19(5)**: 163-71.
- Cotman, C.W., Monaghan, D.T., Ottersen, O.P., Storm-Mathisen, J. (1987) Anatomical organization of excitatory amino acid receptors and their pathways. *TINS* **10**: 273-280
- Danbolt, N.C., Pines, G., Kanner, B.I. (1990) Purification and reconstitution of the sodium- and potassium-coupled glutamate transport glycoprotein from rat brain. *Biochemistry.* **29(28)**: 6734-40.
- Danbolt, N. C. (2001) Glutamate uptake. *Prog. Neurobiol.* **65**: 1-105.
- DeFelice, L.J., Adams, S.V., Ypey, D.L. (2001) Single-file diffusion and neurotransmitter transporters: Hodgkin and Keynes model revisited. *Biosystems.* **62(1-3)**: 57-66.

- Deguchi, Y., Yamato, I., Anraku, Y. (1989) Molecular cloning of *gltS* and *gltP*, which encode glutamate carriers of *Escherichia coli* B. *J Bacteriol.* **171**(3): 1314-9.
- Dehnes, Y., Chaudhry, F. A., Ullensvang, K., Lehre, K. P., Storm-Mathisen, J., Danbolt, N. C. (1998) The glutamate transporter EAAT4 in rat cerebellar Purkinje cells: A glutamate-gated chloride channel concentrated near the synapse in parts of the dendritic membrane facing astroglia. *J. Neuroscience* **18**: 3606-3619.
- Dingledine, R., Borges, K., Bowie, D., Traynelis, S. F. (1999) The glutamate receptor ion channels. *Pharmacol. Rev.* **51**: 7-61.
- Durand, G. M., Kovalchuk, Y., Konnerth, A. (1996) Long-term potentiation and functional synapse induction in developing hippocampus. *Nature* **381**: 71-75.
- Eliasof, S., Arriza, J. L., Leighton, B. H., Amara, S. G., Kavanaugh, M. P. (1998a) Localization and function of five glutamate transporters cloned from the salamander retina. *Vision Res.* **38**: 1443-1454.
- Eliasof, S., Arriza, J. L., Leighton, B. H., Kavanaugh, M. P., Amara, S. G. (1998b) Excitatory amino acid transporters of the salamander retina: identification, localization, and function. *J. Neurosci.* **18**: 698-712.
- Erecinska M, Wantorsky D, Wilson DF. (1983) Aspartate transport in synaptosomes from rat brain. *J. Biol. Chem.* **258**(15): 9069-77
- Fairman, W. A., Vandenberg, R. J., Arriza, J. L., Kavanaugh, M. P., Amara, S. G. (1995) An excitatory amino-acid transporter with properties of a ligand-gated chloride channel. *Nature* **375**: 599-603.
- Finan, T. M., Oresnik, I., Bottacin, A. (1988) Mutants of *Rhizobium meliloti* defective in succinate metabolism. *J. Bacteriol.* **170**: 3396-3403.
- Finan, T. M., Wood, J. M., Jordan D. C. (1981) Succinate transport in *Rhizobium leguminosarum*. *J. Bacteriol.* **148**: 193-202.

- Fonnum, F. (1984) Glutamate: a neurotransmitter in mammalian brain. *J. Neurochem.*, **42**: 1-11.
- Fukuhara, Y., Turner, R.J. (1984) The static head method for determining the charge stoichiometry of coupled transport systems. Applications to the sodium-coupled D-glucose transporters of the renal proximal tubule. *Biochim. Biophys. Acta.* **770(1)**: 73-8.
- Furuta, A., Martin, L. J., Lin, C. L., Dykes-Hoberg, M., Rothstein, J. D. (1997) Cellular and synaptic localization of the neuronal glutamate transporters excitatory amino acid transporter 3 and 4. *Neuroscience* **81**: 1031-1042.
- Fyk-Kolodziej, B., Qin, P., Dzhagaryan, A., Pourcho, R. G. (2004) Differential cellular and subcellular distribution of glutamate transporters in the cat retina. *Visual Neuroscience* **21**: 551-565.
- Gaillard, I., Slotboom, D. J., Knol, J., Lolkema, J. S., Konings, W. N. (1996) Purification and reconstitution of the glutamate carrier GltT of the thermophilic bacterium *Bacillus stearothermophilus*. *Biochemistry* **35(19)**: 6150-6.
- Gendreau, S., Voswinkel, S., Torres-Salazar, D., Lang, N., Heidtmann, H., Detro-Dassen, S., Schmalzing, G., Hidalgo, P., Fahlke, Ch. (2004) A trimeric quaternary structure is conserved in bacterial and human glutamate transporters. *J. Biol. Chem.* **279**: 39505-39512.
- Grewer, C., Balani, P., Weidenfeller, C., Bartusel, T., Tao, Z., Rauen, T. (2005) Individual subunits of the glutamate transporter EAAC1 homotrimer function independently of each other. *Biochemistry.* **44(35)**: 11913-23.
- Grewer, C., Watzke, N., Rauen, T., Bicho, A. (2003) Is the glutamate residue Glu-373 the proton acceptor of the excitatory amino acid carrier 1? *J. Biol. Chem.* **278(4)**: 2585-92
- Halpern, Y. S., Lupo, M. (1965) Glutamate transport in wild-type and mutant strains of *Escherichia coli*. *J. Bacteriol.* **90**: 1288-1295.

- Halpern, Y. S., Barash, H., Dover, S. and Druck, K. (1973) Sodium and potassium requirements for active transport of glutamate by *Escherichia coli* K-12. *J. Bacteriol.* **114**: 53-58.
- Hanahan, D. (1983) Studies on transformation of *Escherichia coli* with plasmids. *J. Mol. Biol.* **166(4)**: 557-80.
- Heginbotham, L., Kolmakova-Partensky, L., Miller, C. (1998) Functional reconstitution of a prokaryotic K⁺ channel. *J. Gen. Physiol.* **111(6)**: 741-9.
- Heyne, R. I., de Vrij, W., Crielgaard, W., Konings, W. N. (1991) Sodium ion-dependent amino acid transport in membrane vesicles of *Bacillus stearothermophilus*. *J. Bacteriol.* **173**: 791-800.
- Hille, B. (1992) Ionic Channels of Excitable Membranes. (272 pp) University of Washington: Sinauer Associates Inc.
- Howland, D. S., Liu, J., She, Y. J., Goad, B., Maragakis, N. J., Kim, B., Erickson, J., Kulik, J., DeVito, L., Psaltis, G., DeGennaro, L. J., Cleveland, D. W., Rothstein, J. D. (2002) Focal loss of the glutamate transporter EAAT2 in a transgenic rat model of SOD1 mutant-mediated amyotrophic lateral sclerosis (ALS). *Proc. Natl. Acad. Sci. USA* **99**: 1604-1609.
- Inage, Y. W., Itoh, M., Wada, K., Takashima, S. (1998) Expression of two glutamate transporters, GLAST and EAAT4, in the human cerebellum: their correlation in development and neonatal hypoxic-ischemic damage. *J. Neuropathol. Exp. Neurol.* **57**: 554-562.
- Kanai, Y., Hediger, M.A. (2003) The glutamate and neutral amino acid transporter family: physiological and pharmacological implications. *Eur. J. Pharmacol.* **479(1-3)**: 237-47. *Review.*
- Kanai, Y., Hediger, M. A. (1992) Primary structure and functional characterization of a high-affinity glutamate transporter. *Nature* **360**: 467-471.

- Kanai, Y., Nussberger, S., Romero, M. F., Boron, W. F., Hebert, S. C., Hediger, M. A. (1995) Electrogenic properties of the epithelial and neuronal high affinity glutamate transporter. *J. Biol. Chem.* **270**: 16561-68
- Kanner, B. I. (1996) Structure/function relationships in glutamate transporters. *Biochem. Soc. Trans.* **24**: 843-846.
- Kanner, B. I., Borre, L. (2002) The dual-function glutamate transporters: structure and molecular characterization of the substrate-binding sites. *Biochim. Biophys. Acta* **1555**: 92-95.
- Kanner, B. I., Sharon, I. (1978) Active transport of L-glutamate by membrane vesicles isolated from rat brain. *Biochemistry* **17**: 3949-3953.
- Kavanaugh, M. P., Bendahan, A., Zerangue, N., Zhang, Y., Kanner, B. I. (1997) Mutation of an amino acid residue influencing potassium coupling in the glutamate transporter GLT-1 induces obligate exchange. *J Biol Chem* **272**: 1703-1708.
- Kekuda, R., Prasad, P. D., Fei, Y. J., Torres-Zamorano, V., Sinha, S., Yang-Feng, T. L., Leibach, F. H., Ganapathy, V. (1996) Cloning of the sodiumdependent, broad-scope, neutral amino acid transporter B0 from a human placental choriocarcinoma cell line. *J. Biol. Chem.* **271**: 18657-18661.
- Kekuda, R., Torres-Zamorano, V., Fei, Y. J., Prasad, P. D., Li, H. W., Mader, L. D., Leibach, F. H., Ganapathy, V. (1997) Molecular and functional characterization of intestinal Na(1)-dependent neutral amino acid transporter B0. *Am. J. Physiol.* **272**: G1463-G1472.
- Knol, J., Veenhoff, L., Liang, W. J., Henderson, P.J., Leblanc, G., Poolman, B. (1996) Unidirectional reconstitution into detergent-destabilized liposomes of the purified lactose transport system of *Streptococcus thermophilus*. *J. Biol. Chem.* **271(26)**: 15358-66.

- Koch, H. P., Larsson, H. P. (2005) Small-scale molecular motions accomplish glutamate uptake in human glutamate transporters. *J. Neurosci.* **25(7)**: 1730-6.
- Komuro, H., Rakic, P. (1993) Modulation of neuronal migration by NMDA receptors. *Science* **260**: 95-97.
- Kück, U. (2005) Heterologe Genexpression. In *Praktikum der Molekulargenetik*. pp. 291-322. Berlin, Heidelberg: Springer.
- Larsson, H. P., Picaud, S. A., Werblin, F. S., Lecar, H. (1996) Noise analysis of the glutamate-activated current in photoreceptors. *Biophys. J.* **70**: 733-742.
- Läuger P. (1979) A channel mechanism for electrogenic ion pumps. *Biochim Biophys Acta.* **552(1)**:143-61.
- Läuger, P. (1980) Kinetic properties of ion carriers and channels. *J. Membr. Biol.* **57(3)**: 163-78. *Review*.
- Levy, L. M., Warr, O., Attwell, D. (1998) Stoichiometry of the glial glutamate transporter GLT-1 expressed inducibly in a Chinese hamster ovary cell line selected for low endogenous Na⁺-dependent glutamate uptake. *J. Neurosci.* **18**: 9620-9628.
- Maduke, M., Pheasant, D. J., Miller, C. (1999) High-level expression, functional reconstitution, and quaternary structure of a prokaryotic ClC-type chloride channel. *J. Gen. Physiol.* **114(5)**: 713-22.
- Masson, J., Sagne, C., Hamon, M., El Mestikawy, S. (1999) Neurotransmitter transporters in the central nervous system. *Pharmacol. Rev.* **51**: 439-464.
- Mayer, L.D., Hope, M.J., Cullis, P.R. (1986) Vesicles of variable sizes produced by a rapid extrusion procedure *Biochim. Biophys. Acta* **858**: 161–168.

- Melzer, N., Biela, A., Fahlke, Ch. (2003) Glutamate modifies ion conduction and voltage-dependent gating of excitatory amino acid transporter-associated anion channels. *J. Biol. Chem.* **278**: 50112-50119.
- Mim, C., Balani, P., Rauen, T., Grewer, C. (2005) The glutamate transporter subtypes EAAT4 and EAATs 1-3 transport glutamate with dramatically different kinetics and voltage dependence but share a common uptake mechanism. *J. Gen. Physiol.* **126**: 571-589.
- Miner, K. M., Frank, L. (1974) Sodium-stimulated glutamate transport in osmotically shocked cells and membrane vesicles of *Escherichia coli*. *J. Bacteriol.* **117**: 1093-1098.
- Mullis, K. B. (1990) *The Unusual Origin of the Polymerase Chain Reaction*. Birkhäuser, Boston.
- Nadler, J. V., Perry, B. W., Cotman, C. W. (1978) Intraventricular kainic acid preferentially destroys hippocampal pyramidal cells. *Nature* **271**: 676-677.
- Pearce, I. A., Cambray-Deakin, M. A., Burgoyne, R. D. (1987) Glutamate acting on NMDA receptors stimulates neurite outgrowth from cerebellar granule cells. *FEBS Lett.* **223**: 143-147.
- Pines, G., Danbolt, N. C., Bjoras, M., Zhang, Y., Bendahan, A., Eide, L., Koepsell, H., Storm-Mathisen, J., Seeberg, E., Kanner, B. I. (1992) Cloning and expression of a rat brain L-glutamate transporter. *Nature* **360**: 464-467.
- Rabacchi, S., Bailly, Y., haye-Bouchaud, N., Mariani, J. (1992) Involvement of the Nmethyl D-aspartate (NMDA) receptor in synapse elimination during cerebellar development. *Science* **256**: 1823-1825.
- Rauen, T. (2000) Diversity of glutamate transporter expression and function in the mammalian retina. *Amino Acids* **19**: 53-62.

- Rigaud, J. L., Pitard, B., Levy, D. (1995) Reconstitution of membrane proteins into liposomes: application to energy-transducing membrane proteins. *Biochim Biophys Acta*. **1231**(3): 223-46. *Review*.
- Robinson, M. B., Coyle, J.T. (1987) Glutamate and related acidic excitatory neurotransmitters: from basic science to clinical application. *FASEB J*. **1**(6): 446-55. *Review*.
- Rossi, D. J., Oshima, T., Attwell, D. (2000) Glutamate release in severe brain ischaemia is mainly by reversed uptake. *Nature* **403**: 316-321.
- Rossi, D. J., Slater, N. T. (1993) The developmental onset of NMDA receptor-channel activity during neuronal migration. *Neuropharmacology* **32**: 1239-1248.
- Rothman, S. (1984) Synaptic release of excitatory amino acid neurotransmitter mediates anoxic neuronal death. *J. Neurosci.* **4**: 1884-1891.
- Rothstein, J. D., Dykes-Hoberg, M., Pardo, C. A., Bristol, L. A., Jin, L., Kuncl, R. W., Kanai, Y., Hediger, M. A., Wang, Y., Schielke, J. P., Welty, D. F. (1996) Knockout of glutamate transporters reveals a major role for astroglial transport in excitotoxicity and clearance of glutamate. *Neuron* **16**: 675-686.
- Rothstein, J. D., Martin, L. J., Kuncl, R. W. (1992) Decreased glutamate transport by the brain and spinal cord in amyotrophic lateral sclerosis. *N. Engl. J. Med.* **326**: 1464-1468.
- Rothstein, J. D., Martin, L., Levey, A. I., Dykes-Hoberg, M., Jin, L., Wu, D., Nash, N., Kuncl, R. W. (1994) Localization of neuronal and glial glutamate transporters. *Neuron* **13**: 713-725.
- Rothstein, J. D., Van Kammen, M., Levey, A. I., Martin, L. J., Kuncl, R. W. (1995) Selective loss of glial glutamate transporter GLT-1 in amyotrophic lateral sclerosis. *Ann. Neurol.* **38**: 73-84.

- Ryan, R. M., Mitrovic, A. D., Vandenberg, R. J. (2004) The chloride permeation pathway of a glutamate transporter and its proximity to the glutamate translocation pathway. *J. Biol. Chem.* **279**: 20742–20751.
- Ryan, R.M., Compton, E.L., Mindell, J.A. (2009) Functional characterization of a Na⁺-dependent aspartate transporter from *Pyrococcus horikoshii*. *J. Biol. Chem.* **284**: 17540-8.
- Schellenberg, G. D., Furlong, C. E. (1977) Resolution of the multiplicity of the glutamate and aspartate transport systems of *Escherichia coli*. *J. Biol. Chem.* **252**: 9055-9064.
- Schwartz, E., Tachibana, M. (1990) Electrophysiology of glutamate and sodium cotransport in a glial cell of the salamander retina. *J. Physiol.* **426**: 43-80.
- Scott, H. L., Pow, D. V., Tannenberg, A. E. G., Dodd, P. R. (2002) Aberrant expression of the glutamate transporter excitatory amino acid transporter 1 (EAAT1) in Alzheimer's disease. *J. Neurosci.* **22**(3): RC206.
- Scott, H. L., Tannenberg, A. E., Dodd, P. R. (1995) Variant forms of neuronal glutamate transporter sites in Alzheimer's disease cerebral cortex. *J. Neurochem.* **64**: 2193-2202.
- Slotboom, D. J., Konings, W. N., Lolkema, J. S. (1999) Structural features of the glutamate transporter family. *Microbiol. Mol. Biol. Rev.* **63**: 293-307.
- Slotboom, D. J., Konings, W. N., Lolkema, J. S. (2001a) Cysteinescanning mutagenesis reveals a highly amphipathic, pore-lining membrane-spanning helix in the glutamate transporter GltT. *J. Biol. Chem.* **276**: 10775-10781.
- Slotboom, D. J., Konings, W. N., Lolkema, J. S. (2001b) The structure of glutamate transporters shows channel-like features. *FEBS Lett.* **492**: 183-186.

- Stallcup, W. B., Bulloch, K., Baetge, E. E. (1979) Coupled transport of glutamate and sodium in a cerebellar nerve cell line. *J. Neurochem.* **32**: 57-65.
- Storck, T., Schulte, S., Hofmann, K., Stoffel, W. (1992) Structure, expression, and functional analysis of a Na⁺-dependent glutamate/aspartate transporter from rat brain. *Proc. Natl. Acad. Sci. USA* **89**: 10955-10959.
- Su, A., Mager, S., Mayo, S. L., Lester, H. A. (1996) A multi-substrate single-file model for ion-coupled transporters. *Biophys J.* **70**(2): 762-777.
- Szatkowski, M., Barbour, B., Attwell, D. (1990) Non-vesicular release of glutamate from glial cells by reversed electrogenic glutamate uptake. *Nature* **348**: 443-45.
- Takeuchi A. (1987) The transmitter role of glutamate in nervous systems. *Jpn. J. Physiol.* **37**(4): 559-72. *Review.*
- Tao, Z., Zhang, Z., Grewer, C. (2006) Neutralization of the aspartic acid residue Asp-367, but not Asp-454, inhibits binding of Na⁺ to the glutamate-free form and cycling of the glutamate transporter EAAC1. *J. Biol. Chem.* **281**(15): 10263-72.
- Tao, Z., Grewer, C. (2007) Cooperation of the conserved aspartate 439 and bound amino acid substrate is important for high-affinity Na⁺ binding to the glutamate transporter EAAC1. *J. Gen. Physiol.* **129**(4): 331-44.
- Tamarappoo, B. K., McDonald, K. K., Kilberg, M. S. (1996) Expressed human hippocampal ASCT1 amino acid transporter exhibits a pH-dependent change in substrate specificity. *Biochim. Biophys. Acta* **1279**: 131-136.
- Tolner, B., Poolman, B., Konings, W. N. (1992) Characterization and functional expression in *Escherichia coli* of the sodium/proton/glutamate symport proteins of *Bacillus stearothermophilus* and *Bacillus caldotenax*. *Mol. Microbiol.* **6**: 2845-2856.

- Tolner, B., Ubbink-Kok, T., Poolman, B., Konings, W. N. (1995a) Cationselectivity of the L-glutamate transporters of *Escherichia coli*, *Bacillus stearothermophilus* and *Bacillus caldotenax*: dependence on the environment in which the proteins are expressed. *Mol. Microbiol.* **18**: 123-133.
- Tolner, B., Ubbink-Kok, T., Poolman, B., Konings, W. N. (1995b) Characterization of the proton/glutamate symport protein of *Bacillus subtilis* and its functional expression in *Escherichia coli*. *J. Bacteriol.* **177**: 2863-2869.
- Turner, R. J. (1985) Stoichiometry of cotransport systems. *Ann N Y Acad Sci.* **456**:10-25. *Review.*
- Utsunomiya-Tate, N., Endou, H., Kanai, Y. (1996) Cloning and functional characterization of a system ASC-like Na(1)-dependent neutral amino acid transporter. *J. Biol. Chem.* **271**: 14883-14890.
- van den Pol, A. N., Gao, X. B., Patrylo, P. R., Ghosh, P. K., Obrietan, K. (1998) Glutamate inhibits GABA excitatory activity in developing neurons. *J. Neurosci.* **18**: 10749-10761.
- Wadiche, J. I., Arriza, J. L., Amara, S. G., Kavanaugh, M. P. (1995) Kinetics of a human glutamate transporter. *Neuron.* **14(5)**: 1019-27.
- Wallace, B., Yang, Y. J., Hong, J. S., Lum, D. (1990) Cloning and sequencing of a gene encoding a glutamate and aspartate carrier of *Escherichia coli* K-12. *J. Bacteriol.* **172(6)**: 3214-20.
- Yamada, K., Watanabe, M., Shibata, T., Tanaka, K., Wada, K., Inoue, Y. (1996) EAAT4 is a post-synaptic glutamate transporter at Purkinje cell synapses. *Neuroreport* **7**: 2013-2017.
- Yernool, D., Boudker, O., Jin, Y., Gouaux, E. (2004) Structure of a glutamate transporter homologue from *Pyrococcus horikoshii*. *Nature* **431**: 811-818.

Zerangue, N., Kavanaugh, M. P. (1996) Flux coupling in a neuronal glutamate transporter. *Nature* **383**: 634-637.

7. Supplemental Information

Table 7.1 Members of the of the DAACS family. From Slotboom *et al.*, 1999.

Name	Organism	Kingdom ^b	Description	No. of residues	Accession no.
ASCT2 Ocu	<i>Oryctolagus cuniculus</i>	E	Neutral-amino-acid transporter	541	O19105
ASCT2 Hs	<i>Homo sapiens</i>	E	Neutral-amino-acid transporter	541	O15758
ASCT2 Mmu	<i>Mus musculus</i>	E	Neutral-amino-acid transporter	553	P51912
ASCT1 Hs	<i>Homo sapiens</i>	E	Neutral-amino-acid transporter	532	P43007
ASCT1 Mmu	<i>Mus musculus</i>	E	Neutral-amino-acid transporter	532	O35874
EAAT1 Tni	<i>Trichoplusia ni</i>	E	Glu/Asp transporter	479	AF003006
EAAT3 Mmu	<i>Mus musculus</i>	E	Glu/Asp transporter	523	P51906
EAAT3 Rno	<i>Rattus norvegicus</i>	E	Glu/Asp transporter	523	P51907
EAAT3 Bta	<i>Bos taurus</i>	E	Glu/Asp transporter	524	O95135
EAAT3 Ocu ^c	<i>Oryctolagus cuniculus</i>	E	Glu/Asp transporter	524	P31597
EAAT3 Hs	<i>Homo sapiens</i>	E	Glu/Asp transporter	524	P43005
EAAT1 Hs	<i>Homo sapiens</i>	E	Glu/Asp transporter	542	P43003
EAAT1 Bta	<i>Bos taurus</i>	E	Glu/Asp transporter	542	P46411
EAAT1 Rno ^c	<i>Rattus norvegicus</i>	E	Glu/Asp transporter	543	P24942
EAAT1 Mmu	<i>Mus musculus</i>	E	Glu/Asp transporter	543	737473
EAAT1 Ati	<i>Ambystoma tigrinum</i>	E	Glu/Asp transporter	543	AF018256
EAAT4 Mmu	<i>Mus musculus</i>	E	Glu/Asp transporter	561	O35544
EAAT4 Rno	<i>Rattus norvegicus</i>	E	Glu/Asp transporter	561	O35921
EAAT4 Hs	<i>Homo sapiens</i>	E	Glu/Asp transporter	564	P48664
EAAT5 Hs	<i>Homo sapiens</i>	E	Glu/Asp transporter	560	O00341
GLT5A Ati	<i>Ambystoma tigrinum</i>	E	Glu/Asp transporter	564	AF018259
GLT5B Ati	<i>Ambystoma tigrinum</i>	E	Glu/Asp transporter	544	AF018260
EAAT2 Hs	<i>Homo sapiens</i>	E	Glu/Asp transporter	572	P43004
EAAT2 Mmu	<i>Mus musculus</i>	E	Glu/Asp transporter	572	P43006
EAAT2 Rno ^c	<i>Rattus norvegicus</i>	E	Glu/Asp transporter	573	P31596
GLT2A Ati	<i>Ambystoma tigrinum</i>	E	Glu/Asp transporter	579	AF018257
GLT2B Ati	<i>Ambystoma tigrinum</i>	E	Glu/Asp transporter	581	AF018258
EAAT Cel	<i>Caenorhabditis elegans</i>	E	Putative Glu/Asp transporter	503	O10901
EAAT Ovo	<i>Onchocerca volvulus</i>	E	Putative Glu/Asp transporter	492	O25605
EAT2 Cel	<i>Caenorhabditis elegans</i>	E	Putative Glu/Asp transporter	532	O21353
EAT3 Cel	<i>Caenorhabditis elegans</i>	E	Putative Glu/Asp transporter	575	O21751
GLT Cel	<i>Caenorhabditis elegans</i>	E	Putative Glu/Asp transporter	491	Z99277
EAT4 Cel	<i>Caenorhabditis elegans</i>	E	Putative Glu/Asp transporter	502	O22682
GltT Bca	<i>Bacillus caldotenax</i>	B	Glu/Asp transporter	421	P24944
GltT Bst	<i>Bacillus stearothermophilus</i>	B	Glu/Asp transporter	421	P24943
YhfG Bsu	<i>Bacillus subtilis</i>	B	Putative Glu/Asp transporter	429	Y14083
GltP Ec	<i>Escherichia coli</i>	B	Glu/Asp transporter	437	P21345
GltP Bsu	<i>Bacillus subtilis</i>	B	Glu/Asp transporter	414	P39817
DctA Ec	<i>Escherichia coli</i>	B	C ₄ -dicarboxylate transporter	428	P37312
DctA Sty	<i>Salmonella typhimurium</i>	B	C ₄ -dicarboxylate transporter	428	P50334
DctA RleN	<i>Rhizobium leguminosarum</i> NGR234	B	C ₄ -dicarboxylate transporter	449	S38912
DctA Sme	<i>Sinorhizobium meliloti</i>	B	C ₄ -dicarboxylate transporter	441	P20672
DctA Rle	<i>Rhizobium leguminosarum</i>	B	C ₄ -dicarboxylate transporter	444	Q01857
YdbH Bsu	<i>Bacillus subtilis</i>	B	Putative C ₄ -dicarboxylate transporter	421	AB001488
DctA Mtu	<i>Mycobacterium tuberculosis</i>	B	Putative C ₄ -dicarboxylate transporter	491	Z81451
b1729 Ec	<i>Escherichia coli</i>	B	Unknown	463	AE000268
YB54 Hin	<i>Haemophilus influenzae</i>	B	Unknown	440	P45079
YhcL Bsu	<i>Bacillus subtilis</i>	B	Unknown	463	P54596
GltP Bbu	<i>Borrelia burgdorferi</i>	B	Unknown	463	AE001172
YgjU Ec	<i>Escherichia coli</i>	B	Serine transporter	414	P42602
YgjU Hin	<i>Haemophilus influenzae</i>	B	Putative serine transporter	414	P45246
GltP Aae	<i>Aquifex aeolicus</i>	B	Unknown	398	AE000735
GltP Ser	<i>Saccharopolyspora erythraea</i>	B	Unknown	449	S71005
GltP Cps	<i>Chlamydia psittaci</i>	B	Unknown	406	AF017105
GltP2 Ctr	<i>Chlamydia trachomatis</i>	B	Unknown	415	AE001296
GltP Tpa	<i>Treponema pallidum</i>	B	Unknown	396	AE001231
GltP2 Tpa	<i>Treponema pallidum</i>	B	Unknown	407	AE001262
GltP2 Bbu	<i>Borrelia burgdorferi</i>	B	Unknown	400	AE001145
GltP Ctr	<i>Chlamydia trachomatis</i>	B	Unknown	412	AE001313
GltP Pho	<i>Pyrococcus horikoshii</i>	A	Unknown	425	AB009510

Table 7.2 Score Table of three distantly related glutamate transporters Glt_{ph}, ecgltP, and hEAAT2.

The table is based on a multiple amino acid sequence alignment using ClustalW (Chenna *et al.*, 2003). Abbreviations: glutamate transporter from archaeobacteria *P. horikoshii* (Glt_{ph}), bacterial glutamate transporter from *E. coli* (ecgltP), and human isoform of excitatory amino acid transporters (hEAAT2).

SeqA	Name	Len(aa)	SeqB	Name	Len(aa)	Score
1	GltPh	425	2	ecgltP	437	33
1	GltPh	425	3	hEAAT2	574	32
2	ecgltP	437	3	hEAAT2	574	26

Table 7.3 List of equipment and materials used.

Equipment / Consumption items	Company
Agarose gel system	PEQLAB Biotechnologie GMBH
Amicon Ultra (Ultracel 30 k)	Millipore
Autoclave Systec D-150	Systec GmbH
Affinity chromatography:	
ÄKTAprime™plus system	GE Healthcare Bio-Sciences
Strep-Tactin® Superflow® High Pressure column	IBA
Cellulose nitrate filter (0.45 µm)	Sartorius Biolab Products
Cuvettes:	
Cuvettes REF 67.742	Sarstedt
UVette 220-1600 nm	Eppendorf
Centrifuges:	
Rotanta 460R Heraeus Fresco 17 centrifuge	Thermo Scientific
Micro centrifuge MiniSpin®	Eppendorf
Table centrifuge 5415C	Eppendorf
Avanti™ J-25 centrifuge	Beckman Coulter, Inc.
Ultracentrifuge Optima™ LE-80k	Beckman Coulter, Inc.
Rotors for the ultracentrifuge: 70 Ti.1, SW-41 TI	Beckman Coulter, Inc.
Centrifuge tubes (15 ml, 30 ml, 50 ml)	Beckman Coulter, Inc.
Centrifuge tubes (15 ml, 30 ml, 50 ml)	G. Kisker GbR
Glass microfiber filters 934-AH™	Whatman
Fast protein liquid chromatography (FPLC) system:	
Superdex column 200 – 10/30	GE Healthcare Bio-Sciences
Optical Unit UV-1	GE Healthcare Bio-Sciences
Pump P-500	GE Healthcare Bio-Sciences
Collector Frac-100	GE Healthcare Bio-Sciences
Recorder Rec 112	GE Healthcare Bio-Sciences
Program GP-250 Plus	GE Healthcare Bio-Sciences
Gel Doc™XR documentation system	BioRad Laboratories GmbH
Glassware	Schott Glaswerke AG
Plasticware	Roth
Illustra NAP-10 Column	GE Healthcare Bio-Sciences
<u>Membrane Extruder for Laboratory:</u>	
LiposoFast-Basic	Avestin Inc.

LiposoFast-Stabilizer	Avestin Inc.
Polycarbonate membrane 400 nm	Avestin Inc.
Hamilton Syringe 1 ml	Hamilton Company
Milli Q plus	Millipore
MillexGP	Millipore
Needle 22G Nr. 12	BD Microlance
Osmomat 030	Gonotec
pH meter 720A	ORION
TRICARB 2800 TR Packard Tri-Carb Liquid Scintillation Counter	PerkinElmer
PCR-Thermocycler T Gradient Thermomixer compact	Biometra
PD-10 Desalting column	GE Healthcare Bio-Sciences
Petri dishes for Bacterial culture (92 x 16 mm, PS)	Sarstedt
Photometer Ultrospec 2100 pro	GE Healthcare Bio-Sciences
Pipettes	Eppendorf
Plastic tubes (1.5 ml, 2 ml)	Eppendorf
Polypropylene tubes (14 ml)	Greiner Bio-One GmbH
Quantamaster 2	PTI
Reaction tubes (0.5 ml, 1.5 ml, 15 ml and 50 ml)	Sarstedt
Reaction tubes (safe lock 1.5 ml, 2 ml)	Greiner Bio-One GmbH
SDS-PAGE system with Power Supply PowerPac™ Basic	BioRad
Spectrophotometer Ultrospec 2100 pro	Amersham Biosciences
Sterile filter Millex-GP Filter Unit	Millipore Corporation
Thermocycler	Biometra or MJ Research
Thermostat Plus system	Eppendorf
Unitron coulter	Infors HT
Ultrasound Sonifier 450	Branson Ultrasonics Corp.
Vacuum concentrator 5301	Eppendorf
Vacuum pump	VACUUBRAND or KNF Neuberger

Table 7.4 List of chemicals used.

Chemicals	Company
Acetic acid (100 %)	Merck
Acetone	Baker
Acrylamide-Bisacrylamide 37.5:1 mixture	SERVA
Agarose	Serva
AHT (anhydrotetracycline hydrochloride)	ACROS ORGANICS
APS (ammonium persulphate)	Serva
Ampicillin, sodium salt	Serva
AMPSO (N-(1,1-Dimethyl-2-hydroxyethyl)-3-amino-2-hydroxypropanesulfonic acid)	Sigma-Aldrich
Aspartic acid, L-[2,3- ³ H]-	MP Biomedicals, Inc.
Bacto™ Agar	Becton, Dickinson and Company
Bio-Beads SM-2 Adsorbent™	BioRad
BSA (bovine serum albumin)	Sigma-Aldrich
Borat sodium salt	Merck
Bromophenol blue sodium salt	AppliChem GmbH
Calcium chloride dihydrate	Merck
dATP (2'-deoxyadenosine 5'-triphosphate)	GE Healthcare Bio-Sciences
Desthiobiotin	Invitrogen
Difco™ LB Broth, Miller (Luria-Bertani)	Becton, Dickinson and Company
di-Sodium hydrogen phosphate dihydrate	Merck
DMF (dimethylformamide)	Sigma-Aldrich
DMSO (dimethylsulfoxide)	Merck
Deoxynucleotide triphosphates (dNTPs): 100 mM dATP, dCTP, dGTP, dTTP	Sigma-Aldrich
DDM (n-Dodecyl-β-maltoside)	GLYCON Biochemicals
DTT (dithiothreitol)	Roth
Decon 90	Decon Laboratories Limited
EDTA (ethylenediaminetetraacetic acid, anhydrous)	Merck
E. coli total Lipid Extract	Avanti Polar Lipids
Ethanol absolute	Baker
Ethidium bromide tablets	USB Corporation

GeneRuler DNA Ladder Mix	Fermentas
Glutamic acid, L-[3,4-3H]-	Hartmann Analytic GmbH
D-Gluconic acid, 45 to 50 wt % solution in water	Sigma-Aldrich
Glycerol (99 %, water free)	KMF Laborchemie Handels GmbH
Glycine	Sigma-Aldrich
Imidazole	Sigma-Aldrich
Isoamyl alcohol	Merck
Isopropanole (2-Propanole)	Merck
HABA (4'-Hydroxyazobenzene-2-carboxylic acid)	Sigma-Aldrich
Potassium acetate extra pure	Merck
Potassium hydrogen phosphate trihydrate	Merck
Liquid nitrogen	Linde
Leupeptin	Serva
Lithium chloride	Serva
Lambda DNA/EcoRI+HindIII marker	Fermentas
Low molecular weight marker (LMW)	GE Healthcare
Sulfuric acid	AppliChem
Magnesium chloride hexahydrate	Merck
Magnesium sulfate	Merck
β -Mercaptoethanol	Serva
Methanol	Baker
MES (morpholinoethanesulfonic acid)	Sigma-Aldrich
NMDG (N-methyl-D-glucamine)	Sigma
PCR-H ₂ O	Braun
PMSF (phenylmethylsulphonylfluoride)	Serva
n-Pentane	Merck
Pepstatin	Serva
Phenol:chloroform:isoamyl alcohol (25:24:1)	Roth
L- α -phosphatidylcholine	Sigma-Aldrich
PIPES (piperazine-N,N'-bis(2-ethanesulfonic acid))	Sigma-Aldrich
HEPES (4-(2-hydroxyethyl)-1-piperazineethanesulfonic acid)	Sigma-Aldrich
Premix ABI PRISM BigDye Terminator v1.1	Applied Biosystems

<u>QIAGEN Kits:</u>	QIAGEN GmbH
Plasmid DNA Purification Kit	
QIAprep Spin Miniprep Kit	
QIAquick Gel Extraction Kit	
QIAquick PCR Purification Kit	
Qiaprep 8 Miniprep Kit	
Qiaprep Spin Miniprep Kit	
Qiagen HiSpeed Plasmid Maxi Kit	
DyeEx 2.0 Spin Kit	
Roti-Blue Colloidal Coomassie staining (5x)	Roth
Hydrochloric acid, HCl (38 %)	Baker
SAM (S-adenosyl methionine)	Sigma-Aldrich
Scintillation cocktail Rotiszint® eco plus	Roth
Silica	Sigma-Aldrich
SDS (sodiumdodecylsulfate)	Merck
Sodium acetate	Merck
Sodium chloride	Merck
Sodium hydrogen phosphate	Merck
Sodium hydroxide	Merck
Sucrose	Baker
Filter-Count LSC-cocktail	PerkinElmer
TCEP (tris(2-carboxyethyl)phosphine hydrochloride)	PIERCE
TEMED (N,N,N',N' tetramethylethylenediamine)	Serva
TRIS (tris(hydroxymethyl)aminomethane)	Merck
Triton X-100	Sigma-Aldrich
Valinomycin	Sigma
Water HPLC quality	Fluka

Table 7.5 Oligonucleotides used. Abbreviations: s = sense, as = antisense.

Construct	s/as	Sequence primer
pASK IBA5 ecglp N401D	s	GAACGTGGTGGGTGATGCGCTGGCGGTG
	as	CACCGCCAGCGCATCACCCACCACGTTC

Table 7.6 Used *Escherichia coli*-strain

<i>E.coli</i> K12:	Genotype
BL-21 (DE3)	F ⁻ , ompT, hsdSβ(rβ-mβ-), dcm, gal, (DE3) tonA
DH5α	F ⁻ , φ80dlacZΔM15, Δ(lacZYA-argF)U169, deoR, recA1, endA1, hsdR17(rk ⁻ , mk ⁺), phoA, supE44, λ ⁻ , thi-1, gyrA96, relA1

8. Acknowledgements

In the first place, I would like to thank my supervisor Prof. Dr. Christoph Fahlke who allowed me to join his group as a PhD student, provided outstanding working conditions, supported me throughout my study and promoted my future as an independent scientist. His constant encouragement and enthusiasm, excellent expertise and stimulating discussions proved invaluable in accomplishing this work. The project that resulted in this thesis was supported by the Deutsche Forschungsgemeinschaft (FOR450) for Ch.F. and P.H.

I am grateful to Prof. Dr. Theresia Kraft and Prof. Dr. Anaclet Ngezahayo for taking the time and effort to read this thesis and taking part in the examination.

My special thanks to Dr. Patricia Hidalgo for very helpful discussions, for creating a very good working atmosphere, and for such great possibilities to learn from her experience. Her thoughtful approach to protein biochemical research was especially educational for me.

Furthermore, I owe my thanks to Dr. Alexi Alekov, Dr. David Ewers, Dr. Martin Fischer, Thomas Gramkow, Dr. Peter-Alexander Kovermann, Dr. Sönke Wimmers, and Dr. Andre Zeug for their contribution and support in glutamate transporter studies, for helpful discussions, and for helping me whenever it was necessary.

I would also like to thank my past and present colleagues for a good working atmosphere, helpful discussions, fruitful cooperations, and help throughout my studies. I would particularly like to thank Birgit Begemann, Petra Kilian, and all my colleagues at the Department of Neurophysiology at the MHH, Mr. Friedemann Scheller and the team of the Department of Nuclear medicine at the MHH, Dr. Dmitry Namgaladze, Patrick Schmidt, Ilinca Ionescu and all my colleagues at the University of Constance and RWTH Aachen.

Next, I wish to thank all my friends all around the world. Especially I would like to thank Dr. Zoryana V. Grishina for her friendship and support. Also I thank Dr. Pen Kay-Jackson, Marie-Luise Endeke, Dr. Kathrin Heinz, Dr. Hennadiy Netuzhylov, Tetyana Zakordonets, Dr. Claudia J. Schulze, Dr. Dmytro Putchkov, and Oksana Dmytriyeva and their families for being a part of my life.

Very special thanks go to my dear parents & grandparents, and to Lea and Zoe, and to our whole family for your unconditional love and support. Thank you for believing in me, standing by me and making it always a pleasure to go home.

9. Curriculum Vitae

Ivanna Shcherbyna

January 20 th 1976	Born in Kyiv, Ukraine.
1991 – 1994	Kyiv Medical College №4. Kyiv, Ukraine.
1995 – 2000	Student of the National Taras Shevchenko University of Kyiv, Biological Department, specialization physiology and ecology of plants. Kyiv, Ukraine.
2000	Graduated as “Magister in Biology, Physiology”.
Jun. 1998 – Aug. 2001	Research assistant position at the Department of Phytohormonology, M. G. Kholodny Institute of Botany, National Academy of Sciences (NAS) of Ukraine. Kyiv, Ukraine.
Oct. 2001 – Sept. 2003	Research position at the Department of Biological Chemistry, Faculty of Biology, University of Konstanz. Konstanz, Germany.
Oct. 2003 – Aug. 2005	Research position at the Department of Physiology, University Hospital Aachen, University of Technology (RWTH) Aachen. Aachen, Germany.
Sept. 2005 – present	Research position at the Department of Neurophysiology, Medical School Hannover (MHH). Hannover, Germany.
Oct. 2008 – present	PhD student of the Gottfried Wilhelm Leibniz University of Hannover, Faculty of Natural Sciences, Biological Department, specialization cell- and developmental biology. Hannover, Germany.

10. List of publications

Publications

- 2009 **I. Shcherbyna**, D. Ewers, P. Hidalgo, Ch. Fahlke. Functional characterization of a glutamate transporter from *E. coli*. (Manuscript in preparation).
- 2005 D. Namgaladze, **I. Shcherbyna**, H. W. Hofer, V. Ullrich (2005). Superoxide targets calcineurin in vascular endothelium. *Biochemical and Biophysical Research Communications* 334, (4): 1061-1067.

Conference Contributions

- 2009 **I. Shcherbyna**, D. Ewers, P. Hidalgo, Ch. Fahlke (2009) Sodium dependence of glutamate transport by a prokaryotic glutamate transporter. *Acta Physiologica* 195, (669): 89. (Oral session, Conf. Proceedings)
- 2009 D. Ewers, T. Becher, **I. Shcherbyna**, P. Hidalgo, Ch. Fahlke (2009) Cation binding to bacterial glutamate transporters characterized through equilibrium and stop flow tryptophan fluorescence. *Acta Physiologica* 195, (669): 131. (Conf. Proceedings)
- 2007 **I. Shcherbyna**, D. Nothmann, D. Ewers, P. Hidalgo, Ch. Fahlke (2007) A bacterial glutamate transporter that functions at variable transport stoichiometry. *Acta Physiologica* 189, (653): 150. (Conf. Proceedings)
- 2006 **I. Shcherbyna**, P. Hidalgo, Ch. Fahlke (2006) Functional Characterization of a Glutamate Transporter from *E. coli*. 50th Annual meeting of the Biophysical Society. Poster Session: Membrane Transporters & Exchangers.

-
- 2005 **I. Shcherbyna**, P. Hidalgo, Ch. Fahlke (2005) Functional characterization of a bacterial glutamate transporter from *E. coli* reconstituted in lipid vesicles. International School of Biophysics, Ettore Majorana Foundation and Center for Scientific Culture. Course "Channels and Transporters. Excitability, Secretion, and Transport: Molecules to Medication".
- 2005 **I. Shcherbyna**, P. Hidalgo, Ch. Fahlke (2005) Functional characterization of bacterial glutamate transporter reconstituted in lipid membranes. *The Ukrainian Biochemical Journal* 77, (2): 75. (Conf. Proceedings)
- 2005 **I. Shcherbyna**, P. Hidalgo, Ch. Fahlke (2005). Functional characterization of a bacterial glutamate transporter from *E. coli*. *Pflügers Archiv European Journal of Physiology*. (Conf. Proceedings)
- 2003 D. Namgaladze, **I. Shcherbyna**, H. W. Hofer, V. Ullrich (2003) Calcineurin is a target of superoxide in mammalian cells. Abstract *EMBO Conference/FEBS Advanced Course EuroPhosphatases*. (Conf. Proceedings)